THE JOURNAL OF BIOLOGICAL CHEMISTRY VOL. 288, NO. 21, pp. 14788–14804, May 24, 2013

A Role for Cargo in Arf-dependent Adaptor Recruitment*

Received for publication, January 15, 2013, and in revised form, April 1, 2013 Published, JBC Papers in Press, April 9, 2013, DOI 10.1074/jbc.M113.453621

Amanda H. Caster[‡], **Elizabeth Sztul**[§], **and Richard A. Kahn**[‡1]

From the [‡]*Department of Biochemistry and the Emory University School of Medicine, Atlanta, Georgia 30322 and the* [§]*Department of Cell, Developmental, and Integrative Biology University of Alabama at Birmingham School of Medicine, Birmingham, Alabama 35294*

Background: Cargo proteins recruit Arf-dependent adaptors for packaging.
Results: Cargo presence at the Golgi/endosomes leads to specific adaptor recruitment.
Conclusion: Arf activation is more closely coupled to cargo than previously appreciated, and we interpret the specificity in adaptor recruitment as evidence of the lack of freely diffusible activated Arfs.
Significance: Cargos play a role in the activation of Arfs and recruitment of specific adaptors.

Membrane traffic requires the specific concentration of protein cargos and exclusion of other proteins into nascent carriers. Critical components of this selectivity are the protein adaptors that bind to short, linear motifs in the cytoplasmic tails of transmembrane protein cargos and sequester them into nascent carriers. The recruitment of the adaptors is mediated by activated Arf GTPases, and the Arf-adaptor complexes mark sites of carrier formation. However, the nature of the signal(s) that initiates carrier biogenesis remains unknown. We examined the specificity and initial sites of recruitment of Arf-dependent adaptors (AP-1 and GGAs) in response to the Golgi or endosomal localization of specific cargo proteins (furin, mannose-6-phosphate receptor (M6PR), and M6PR lacking a C-terminal domain M6PRΔC). We find that cargo promotes the recruitment of specific adaptors, suggesting that it is part of an upstream signaling event. Cargos do not promote adaptor recruitment to all compartments in which they reside, and thus additional factors regulate the cargo's ability to promote Arf activation and adaptor recruitment. We document that within a given compartment different cargos recruit different adaptors, suggesting that there is little or no free, activated Arf at the membrane and that Arf activation is spatially and temporally coupled to the cargo and the adaptor. Using temperature block, brefeldin A, and recovery from each, we found that the cytoplasmic tail of M6PR causes the recruitment of AP-1 and GGAs to recycling endosomes and not at the Golgi, as predicted by steady state staining profiles. These results are discussed with respect to the generation of novel models for cargo-dependent regulation of membrane traffic.

Members of the ADP-ribosylation factor (Arf)[2] family of regulatory GTPases, within the larger Ras superfamily, play fundamental roles in the regulation of membrane traffic at multiple sites in all eukaryotes, including at least the Golgi, endosomes, endoplasmic reticulum (ER), ER-Golgi intermediate compartments, and plasma membrane. Probably the most completely characterized is Sar1, the most divergent member of the Arf family, and its role in recruitment of the COPII coat to nascent buds emanating from the ER (1, 2). A far more complicated picture emerges for the specific roles of the Arfs in the regulation of membrane traffic at the Golgi and endosomes. At these sites multiple Arfs (Arf1–5) have been implicated as regulators with at least some level of redundancy in functions (3). The best known of these functions is the direct recruitment of soluble protein adaptors that also bind directly to linear motifs present in the cytosolic "tails" of transmembrane protein "cargos" (4, 5). Perhaps the most vivid demonstration of this is through the use of the drug brefeldin A (BFA), which prevents Arf activation by direct binding and inhibition of a subset of the Arf guanine nucleotide exchange factors (GEFs) and causes rapid release of Arf-dependent adaptors in live cells. However, Arfs have also been shown to directly bind and/or activate phospholipase D, phosphatidylinositol 4-kinase, and phosphatidylinositol 4-phosphate 5-kinase (6–8). It is the combination of functional redundancy and multiplicity of effectors that has made dissection of signaling demanding and resulted in delays in advance of molecular models of the mechanisms of Arf actions. Even more importantly, we still lack a fundamental understanding of what spatially regulates Arf activities and thus struggle to understand the role of Arf in membrane traffic.

Like all regulatory GTPases, Arfs act in cells as molecular switches, toggling between activated (GTP-bound) and inactivated (GDP-bound) states. These different states are conformational and result in different affinities for binding partners, notably the effector proteins that lead to the generation of the biological response. Inter-conversion between conformational states is controlled by the actions of GEFs, which promote the rate-limiting dissociation of GDP and allow GTP to bind and activate the GTPase. Conversely, return to the inactive state is controlled kinetically by the actions of GTPase-activating proteins, which increase the rate of GTP hydrolysis by the GTPase.

* This work was supported, in whole or in part, by National Institutes of Health Grant GM067226 (NIGMS) and by Imaging Core of the Emory Neuroscience NINDS Core Facilities Grant P30NS055077.

[1] To whom correspondence should be addressed: Dept. of Biochemistry, Rollins Research Center, Emory University, 1510 Clifton Ave., Suite G-218, Atlanta, GA. Tel.: 404-727-3561; E-mail: rkahn@emory.edu.

[2] The abbreviations used are: Arf, ADP-ribosylation factor; ER, endoplasmic reticulum; BFA, brefeldin A; GEF, guanine nucleotide exchange factor; M6PR, mannose 6-phosphate receptor; NRK, normal rat kidney; 3D3I, three-dimensional image-based isosurface intensity analysis; TfR, transferrin receptor; TGN, *trans*-Golgi network.

The heterotrimeric G proteins are paradigms for regulatory GTPase signaling and use G protein-coupled receptors, which act directly as G protein GEFs, to acutely and locally activate G proteins in response to ligand binding (9). This binding initiates signaling by G proteins, with consequent changes in effector activation and generation of second messengers. Even a cursory review of the history of G protein research reveals that knowledge of the ligand as an initiator of signaling and the ability to acutely activate G protein signaling allowed researchers to identify components that are required for signal generation and modulation. In addition, the use of different ligands allowed clear descriptions of the sources of specificity in G protein signaling. Similarly, ligand binding to receptor-tyrosine kinases can result in phosphorylation of specific residues in the cytoplasmic tails that act as binding sites for Grb2/SOS, which is a Ras GEF (9). Thus, paradigms for activation of regulatory GTPases are found within these two homologous systems in which ligand binding to transmembrane proteins leads to localized activation of a GEF activity and consequently the activation of a specific and narrow subset of cellular GTPases. In contrast, despite more than 25 years of research into Arf biology, we still do not know the initiator of signaling or whether the process is initiated via a "ligand equivalent" or if it may be constitutive. To begin to address this central question of Arf biology we developed a cell-based model for Arf activation using the best characterized Arf effectors, the Arf-dependent adaptors.

Adaptors are soluble proteins or protein complexes that are recruited to membranes through direct binding to activated Arf and to sorting signals in transmembrane proteins, which we term cargos. The function of adaptor recruitment is the initiation of formation of a coated bud, later maturing into a carrier, that (i) concentrates cargo by binding specific sorting signals, (ii) deforms planar bilayers into tubes and carriers, (iii) and recruits accessory proteins required for carrier maturation, scission, binding to cytoskeletal elements, targeting to and destination membranes, and initiating uncoating and fusion at that site (4, 10–13). At least eight of these Arf-dependent adaptors have been reported to be recruited to Golgi membranes by activated Arf(s), and each has been described as binding distinctive sorting motifs; the heptameric COPI complex binds KK*XX* (14, 15) and FF motifs (16, 17), GGAs1–3 bind D*XXX*LL (18), Mint3 binds the YENP*X*Y motif (19), and adaptins (AP-1-AP-4) bind the Y*XXϕ* (20) and *XXX*LL (21) motifs. Each of these Arf-dependent adaptors is soluble and present in cytosol until recruited to the membrane of budding carriers by activated Arfs. Arfs also reside in cytosol and are recruited to membranes through hydrophobic interactions involving the amphipathic N-terminal α-helix and covalently attached N-terminal myristate (22). The association of Arfs with membranes is tightly linked to their activation, exchange of GDP for GTP, catalyzed by an Arf GEF. Thus, monitoring Arf recruitment to membranes might be one way to assay for their activation in cells. However, we lack antibodies capable of recognizing specific Arfs on membranes. In addition, there have been well documented concerns over the use of tagged Arfs or fusion proteins (23). Thus, to begin the search for factors that lead to Arf GEF activation in cells, we use Arf-dependent adaptor recruitment as an indirect assay for Arf activation in cells.

Because specific adaptors have been associated in the literature with specific transmembrane cargos and at specific sites in cells, we chose a set of cargos for our cell-based assays that would provide overlapping but also specific differences in adaptor recruitment; specifically, the cation-independent, mannose 6-phosphate receptor (M6PR) and furin. These are previously characterized single pass, type I transmembrane proteins that bind directly to overlapping sets of adaptors via previously defined sorting signals. M6PR binds to AP-1 and GGAs in what has widely been interpreted as a requirement for its anterograde traffic from the Golgi to the endosome (24, 25). The M6PR has been extensively studied as a model for bi-directional Golgi-endosome traffic (26–30). M6PRs act in cells to transport soluble, lumenal, mannose 6-phosphate-modified hydrolases from the Golgi to their site of action in lysosomes. The binding site for GGAs on the M6PR C-terminal, cytoplasmic tail is known, allowing members of the Robinson laboratory (31) to generate a truncation mutant, M6PRΔC, that retains AP-1 binding but has lost the ability to recruit GGAs. M6PRs are found predominantly on Golgi, endosomal, and plasma membranes with different steady state distributions in different cell types. Furin is a protease that cleaves proteins at RR/KK motifs within the Golgi lumen (for review, see Thomas (32)). It is localized predominantly to the Golgi but can escape to endosomes, where it may also function before retrieval back to the Golgi. Furin contains within its cytoplasmic tail a sorting sequence that binds directly to AP-1 (33). This interaction has been reported to be responsible for the export of furin from the Golgi to endosomes (33). Furin can also bind to Mint3 (34). Mint3 binds the cytoplasmic tail of furin at the Golgi, but it acts to retain furin there (34).

We originally chose to focus our studies on adaptor recruitment to the Golgi. Focusing on this location allowed us to take advantage of two well characterized protocols that affect cargo traffic there: low temperature incubation (20 °C) serves as a kinetic block of export from the Golgi (35–38) and BFA treatment that causes the rapid and reversible loss of Arf-dependent adaptors from membranes (39–41). Our data confirm the specificities of cargo tail-adaptor interactions established previously from *in vitro* binding data and highlight important differences in the sites of adaptor recruitment by different cargos.

EXPERIMENTAL PROCEDURES

Cell Culture—HeLaM and normal rat kidney (NRK) cells were maintained in 10% fetal bovine serum (GemCell catalog #100–500, Sacramento, CA) in DMEM medium (Invitrogen catalog #11965). Stably transfected cells were supplemented with 50 μg/ml G418. Cells used for imaging were grown on Matrigel-coated coverslips (BD Biosciences).

Plasmids and Cell Transfections—pIRESneo2-CD8-M6PR and pIRES-neo2-CD8- M6PRΔC were generous gifts from Dr. Margaret Robinson (University of Cambridge) and are described in Hirst *et al.* (31). They express the lumenal and transmembrane regions of CD8 fused to the full 163 residues of the cytoplasmic tail of cation-independent M6PR or only the juxtamembrane 74 residues, respectively. pIRESneo2-CD8-fu-

rin was kindly provided by Dr. Matthew Seaman (University of Cambridge). The cytoplasmic tail of furin is 58 residues in length. pGEM FLAG-furin was a generous gift from Dr. Gary Thomas (Oregon Health and Science University) (42). Plasmids were transfected using FuGENE 6 (Roche Applied Science catalog #11814443001) according to manufacturer's instructions. Cells were placed at 37 °C for 4 h, rinsed once, and trypsinized to remove them from the well. Cells were suspended in 3 ml of normal growth medium, and 1 ml of the suspension was transferred to a new well of 6-well plates containing Matrigel-coated coverslips. Cargos were allowed to express for a total of 24 h.

Antibodies and Dilutions Used for Immunocytochemistry—Antibodies and dilutions were: γ-Adaptin (AP-1), 1:100 (BD Transduction Laboratories catalog #610502); CD8, 1:1000 (Ancell Corp. catalog #153-020 Bayport, MN); CD8-FITC, 1:500 (Ancell Corp. catalog #153-040), GGA1 1:1000 (Boman *et al.* (61)); giantin, 1:1000 (Covance catalog #prb-114c Emeryville, CA); GM130, 1:1000 (BD Transduction Laboratories catalog #610823); FAPP2, 1:1000 (D'Angelo *et al.* (84)), a generous gift from Dr. Antonella de Matteis; TGN46, 1:1000 (Serotec catalog #AHP500 Oxford, UK); Rab11, 1:200, a kind gift from Dr. James Goldenring (85); transferrin receptor, 1:1000 (Zymed Laboratories Inc. catalog #136800 Carlsbad, CA); Mint3, 1:100 (BD Transduction Laboratories catalog #611380). Antibodies and dilutions used in immunoblotting were: γ-adaptin, 1:100 (BD Transduction Laboratories catalog #610502); GGA1, 1:500 (Boman *et al.* (61)); Mint3, 1:500 (BD Transduction Laboratories catalog #611380).

Temperature (20 °C) Block and Immunocytochemistry—Medium was replaced with 4 ml of 20 mM HEPES, 10% FBS in DMEM. Cells were placed in a water bath and maintained at 19.5 °C for 4 h, then either immediately fixed or returned to 37 °C for varying times of "release" before fixation. Release was performed by replacing medium with fresh, prewarmed (37 °C) medium without HEPES, and dishes were placed in a gassed incubator. Cells were fixed in 2% paraformaldehyde in phosphate-buffered saline (PBS; 137 mM NaCl, 2.7 mM KCl, 10 mM Na_2HPO_4, 2 mM KH_2PO_4, pH 7.4) for 20 min at room temperature. After fixation, cells were rinsed with PBS for 5 min a total of 4 times. Individual coverslips were then placed on a Parafilm-coated 24-well dish, and ~200 μl of blocking solution (1% bovine serum albumin (BSA, Sigma catalog #A3059) and 0.05% saponin (Sigma #S5881) in PBS) for 20 min at room temperature. Primary antibodies in blocking solution were added to coverslips and placed at 4 °C overnight. Coverslips were then washed 4 times with 0.05% saponin in PBS for 5 min each. Coverslips were mounted using Mowiol (Calbiochem #475904) prepared as described in Valnes and Brandtzaeg (43).

BFA Treatment—BFA (7.5 μg/ml) or methanol vehicle were prepared freshly in culture medium, prewarmed to 37 °C, and applied to cells for 2 min. Cells were then quickly rinsed with prewarmed medium, and fresh medium was applied before fixing as above.

Confocal Image Acquisition—Images were collected on an Olympus IX81 Fluoview FV1000 using a 100× oil immersion objective with a NA of 1.4. Images were imported into ImageJ and converted to 16-bit images, and intensities were scaled to a maximal signal intensity of 255 (44, 45).

Wide Field Image Acquisition—Stacks of images were collected using a Nikon Bx51 microscope with a 60 × 1.4NA oil immersion objective with a Photometrics Quantix camera. Images were captured at 1316 × 1035 pixel ratio and a 16-bit image depth. Where indicated, z-series were deconvolved with Huygens SVI software (Hilversum, The Netherlands) using an iterative maximum likelihood function for a maximum of 40 iterations.

Wide Field Image Quantification—We developed a method for the quantification of three-dimensional-wide field fluorescence data that identifies structures and evaluates signal intensity information within those structures and named the technique three-dimensional ***i***mage-based ***i***sosurface generation and ***i***ntensity analysis (3D3I). The 3D3I method differs from traditional co-localization methods of quantification. Co-localization methods typically use two-dimensional datasets and a manually defined region of interest for analysis. The region of interest is then analyzed for how well signal in one channel correlates with signal in another. In contrast, 3D3I establishes a region of interest, or three-dimensional isosurface, using a biologically relevant signal from one channel (*e.g.* giantin staining) and quantifies the total intensity of signal from the other channel (*e.g.* adaptor staining) within it. Thus, the values generated (intensity per μm^3) are non-correlative. For additional details and discussion see Caster and Kahn (46). The use of 3D3I eliminates the potential for focal plane bias by using data from the entire cell. It is optimal for quantifying staining in irregularly shaped objects, particularly ones that differ in size and number between cells in a population; *e.g.* Golgi components and endosomes.

Deconvolved images were opened in Imaris (Bitplane, South Windsor, CT), and isosurfaces were generated for the staining of interest. Isosurfaces representing Golgi or cargo staining were generated using "automatic iterative selection." The total fluorescence intensity of the channel of interest was then totaled within the volume defined by the isosurface. Values were then exported into Excel for each individual cell. At least five cells were quantified in each case.

Statistical Analysis—Sum intensities from the channel of interest were totaled and divided by the total volume of the surface, resulting in a ratio of sum intensity/isosurface μm^3. This value was determined for each cell for statistical analysis. One-way analysis of variance or Student's *t* test was used with the indicated post-test. Every experiment described was repeated at least three times with consistent results. Images shown are representative of the cell population, determined by quantification of the phenotypes observed.

RESULTS

To identify the signal(s) leading to Arf activation we sought to develop cell-based assays for Arf activation that are spatially and temporally restricted, as expected for biologically relevant processes. Because the Arfs and adaptors reside in excess in cytosol, we expect that the transmembrane cargos will be limiting for generation of the cargo-adaptor-Arf complexes. To ensure that the cargo-dependent adaptor recruitment being studied results primarily or exclusively from cytoplasmic surface interactions, we performed studies using fusion proteins

made up of the lumenal and transmembrane domains of CD8 fused to the cytoplasmic tails of furin or M6PR, termed CD8-furin and CD8-M6PR, respectively. The value of such CD8 fusion proteins has been demonstrated by previous work in the laboratories of Robinson (31) and Seaman (31, 47, 48). We obtained from them the CD8-M6PR plasmid and a C-terminal truncation mutant of CD8-M6PR, termed CD8-M6PRΔC, that retains binding to AP-1 but has lost the GGA binding motif and ability to recruit GGAs (Ref. 31 and see below). To ensure that the CD8 fusion proteins are indeed representative of the full-length proteins we also performed the same studies using either an N-terminal fusion of green fluorescent protein (GFP) and M6PR (GFP-M6PR) or N-terminal FLAG-tagged furin (FLAG-furin). HeLaM cells were used in most of our studies because they are adherent, flat, and display low levels of perinuclear adaptor staining, facilitating imaging of cargo-dependent adaptor recruitment. The availability of stably transfected HeLaM cells expressing CD8-M6PR or CD8-M6PRΔC also provided a useful control for potential artifacts resulting from the more variable levels of expression seen after transient transfections. Each of the major findings described below was confirmed using these stably transfected cells.

Cargo Defines the Specificity of Arf-dependent Adaptor Recruitment—HeLaM cells were transiently transfected with plasmids encoding CD8-furin, CD8-M6PR, or CD8-M6PRΔC and analyzed by indirect immunofluorescence for the effects of cargo expression on adaptor recruitment. Conditions were chosen to minimize the level of protein expression (see "Experimental Procedures"); *e.g.* only those cells displaying minimal but clear evidence of protein expression were chosen for analyses. Immunoblotting of total cell lysates revealed that each of the CD8 fusion proteins was expressed to similar levels (not shown).

Expression of the three cargos resulted in specific profiles of adaptor recruitment. The expression of CD8-furin (Fig. 1*A*) or FLAG-furin (data not shown) led to the specific recruitment of AP-1 and Mint3 but not GGA1. Expression of CD8-M6PR (Fig. 1*A*) or GFP-M6PR caused specific increases in the perinuclear staining of AP-1 and GGA1 (Fig. 1*A*, *C*) but not Mint3, whereas expression of CD8-M6PRΔC led to increases in AP-1 staining but not that of GGA1 or Mint3 (Fig. 1*A*). We also stained fixed cells for GGA2 and GGA3, and in each case they behaved qualitatively the same as described for GGA1 (data not shown). Transient transfection resulted in cells with varying levels of expression of M6PR or CD8-M6PR within a cell population, and we noted by visual inspection a good correlation between the levels of cargo expression and levels of recruitment of AP-1 and GGAs, with no changes to staining of Mint3, even in cells expressing the highest levels of cargo. HeLaM cells stably transfected with CD-M6PR or CD8-M6PRΔC resulted in adaptor recruitment profiles identical to those seen using transient transfections. The data shown in Fig. 1*A* are single cell representatives of the consequences on adaptor recruitment from specific cargo expression. The detailed and rigorous quantification of these responses is described below.

Thus, the cell-based assay for cargo-dependent adaptor recruitment faithfully recapitulates the specificity with which sorting motifs in the cytoplasmic tails of these cargos bind

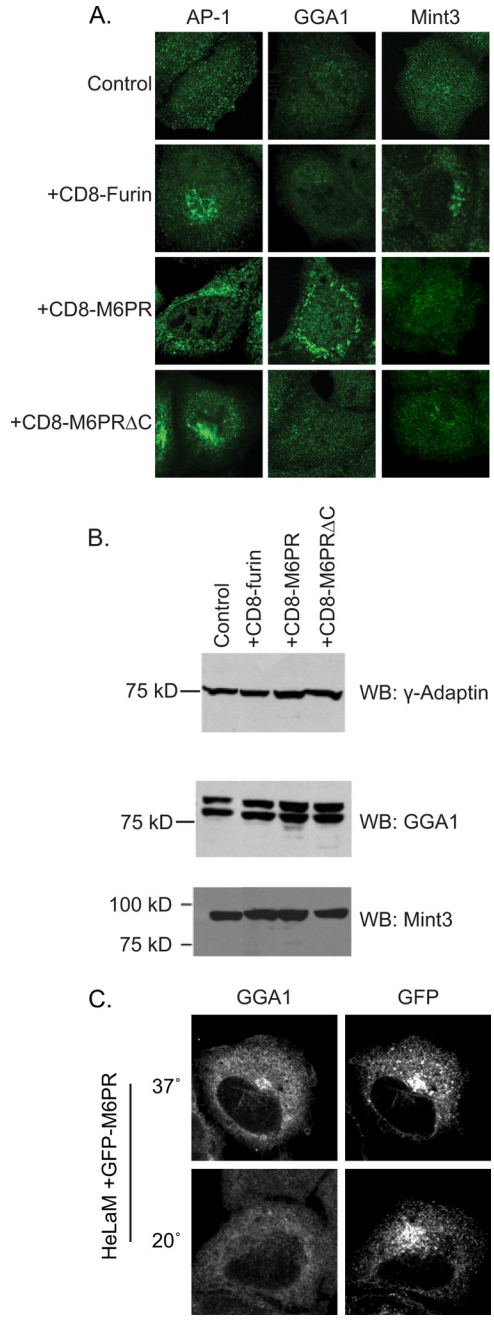

FIGURE 1. **Cargo expression increases the recruitment of specific Arf-dependent adaptors to membranes.** *A*, HeLaM cells were transiently transfected with empty vector (Control) or plasmids directing expression of the indicated cargo. The next day cells were fixed and stained for γ-adaptin (*AP-1*), GGA1, or Mint3. Confocal images are shown. *B*, HeLaM cells were transiently transfected with plasmids that express the indicated cargos before analyzing protein expression by immunoblotting (*WB*) for γ-adaptin, GGA1, or Mint3. GGA1 migrates as a doublet, presumably resulting from post-translational modification, *e.g.* phosphorylation. Results shown are typical of five independent experiments. *C*, HeLaM cells expressing GFP-M6PR were maintained at 37 °C or at 20 °C for 4 h. Cells were then fixed and stained with antibodies against GFP and GGA1. GGA1 recruitment was comparable to that seen with CD8-M6PR and was lost during the temperature block.

adaptors *in vitro* (49–51). Importantly, in every experiment described herein, we did not observe a change in the endogenous levels of the adaptors being studied, as determined by immunoblotting of total cell lysates for γ-adaptin (a component of AP-1), GGA1, and MINT3 (Fig. 1*B*). Thus, we interpret the

increased staining of each adaptor at a membrane surface to result from its recruitment from a cytosolic pool and not from a change in expression levels. Together, these results suggest that cargo levels modulate activation of Arfs and subsequent adaptor recruitment, positioning cargo upstream in the activation pathway. Our data suggest that cargo-mediated activation of Arfs is restricted in the sense that no free Arf is produced to recruit non-relevant adaptor, *i.e.* although CD8-M6PR activates Arfs, those Arfs only recruit AP-1 and GGA1 but not Mint3. Thus, the activated Arfs function within the context of the cargo responsible for its activation. Unfortunately, technical limitations currently prohibit us from identifying which Arfs are involved in each adaptor recruitment and whether they differ with cargo.

To further confirm that recruitment of Arf-dependent adaptors and their responsiveness to different perturbations are consistent between full-length cargos and their CD8-fusion constructs, we compared results with an N-terminal-tagged form of full-length M6PR (Fig. 1*C*). GFP-M6PR expression resulted in increased GGA1 (Fig. 1*C*) and AP-1 (data not shown) recruitment to the Golgi. As fixation can affect the ability of GFP to fluoresce, we indirectly labeled cells expressing GFP-M6PR by staining them with a primary antibody against GFP using a secondary antibody conjugated to Alexa 405, allowing us to image GFP-M6PR on a channel distinct from the GFP excitation/emission profile (488 nm/519 nm, respectively). Cells were chosen for imaging if they showed low levels of GFP expression on both the 405- and 488-nm channels. The GFP-M6PR-dependent recruitment of GGA1 (Fig. 1*C*) or AP-1 (data not shown) to the Golgi was lost in response to a 20 °C temperature block as described in detail below. Thus, these properties and others reported below were consistent throughout for both full-length proteins and the CD8 fusions of the paralogous cargo.

Cargos Localize Differently within the Endomembrane System and within the Golgi—The adaptor recruitment shown in Fig. 1*A* was quite striking and unambiguous. Despite this, and to be able to compare results with different cargos and to determine sites of recruitment for adaptors that potentially act at more than one site, we developed protocols for quantifying adaptor recruitment. Because the Golgi and endosomes are irregular structures that can appear quite different between cells and in different focal planes of the same cell, we sought a method that is inclusive of all staining in each cell and is not subject to focal plane bias. We used 3D3I analysis (46) that employs wide field imaging with deconvolution and Imaris software to quantify overlap of staining of any two antigens in fixed cells. In our studies we used 3D3I to generate isosurfaces defined by cargo or organelle marker staining and determined the extent to which adaptor or cargo staining is included in those defined isosurfaces. Results are expressed as a ratio of total pixel intensity of adaptor or cargo per unit volume of isosurface (defined by the cargo or marker) from each cell in units of sum staining intensity/μm^3. This method has a number of advantages; 1) isosurfaces are defined by a biologically relevant marker, 2) we monitor changes in co-localization throughout the entire volume of the cell and thus avoid sampling or focal plane bias, 3) we perform statistical analyses on a number of cells, comparing intensity per unit volume in control *versus* experimental conditions, as opposed to performing statistical analysis on mean correlation scores. We note that this method yields -fold differences that are typically smaller than those from simple pixel overlap approaches and that statistical testing allows high confidence in the conclusions.

To determine the location of each cargo at steady state (defined herein as HeLaM cells fixed 24 h after transfection and maintained throughout at 37 °C) we quantified the overlap of each cargo with that of a number of markers of the Golgi/*trans*-Golgi network (TGN) and endosomal compartments. The Golgi is a heterogeneous compartment with at least three regions, defined relative to import and export sites as cis-, medial-, and trans-Golgi, with the TGN emerging from this last compartment and typically not resolved from the trans-Golgi at the level of light microscopy. We used p115 or GM130, giantin, mannosidase II, and TGN46 as previously characterized markers of the early, middle, and late Golgi/TGN compartments.

When we compared the localization of each cargo to that of the different Golgi markers, we found some marked and surprising differences. At steady state, most (71.3 ± 14.8%) CD8-furin staining was found within TGN46 isosurfaces, with 51.3 ± 11.7% also within giantin isosurfaces (Fig. 2*A*, *filled bars*). This reveals localization to multiple compartments but with a clear bias toward the TGN. Note that the sum can be greater than 100% when the markers themselves overlap. In contrast, only 19.0 ± 6.4% of all CD8-M6PR staining was found within TGN46 isosurfaces and 25.9 ± 15.4% within giantin isosurfaces in cells maintained at 37 °C (Fig. 2*A*, *filled bars*). This indicates that CD8-M6PR is more widely distributed and less concentrated in parts of the late Golgi/TGN containing these markers than is CD8-furin. These data were obtained from images such as those shown in Fig. 2*B*, where cells were stained for the cargos, and Golgi markers are indicated. Isosurfaces were generated for both the cargo and the Golgi marker. The cargo was falsely colored as a red/yellow heat map based on the amount of Golgi marker also present within the cargo isosurface (Fig. 2*B*, *scale is shown on the right edge*). The Golgi marker is displayed in *green*. CD8-furin is biased toward the TGN (compare the amount of *yellow* in the *upper left panel versus the right*), whereas CD8-M6PR is more evenly distributed within giantin- and TGN46-labeled compartments (compare the *lower left versus right panels*). These results are consistent with previously described roles for furin as an endopeptidase that localizes to the Golgi and is predominantly retained there and for M6PR as a carrier for lysosomal enzymes that cycles between the Golgi and TGN/endosomal compartments.

For comparison, we also used the more common measures of co-localization by evaluating the distribution of CD8-M6PR within the Golgi by comparing the overlap (Mander's coefficients) of cargo staining from a single plane of a confocal image with markers of early (p115), medial (mannosidase II), and late (TGN46) Golgi (Fig. 2*C*). This method of quantification essentially serves as a coincidence detector, indicating the co-localization of a Golgi marker and cargo signals. Using this approach, CD8-M6PR showed more overlap with TGN46 than it did with early or medial Golgi markers (p115 and mannosidase II, respectively). Thus, there is a clear bias of CD8-M6PR

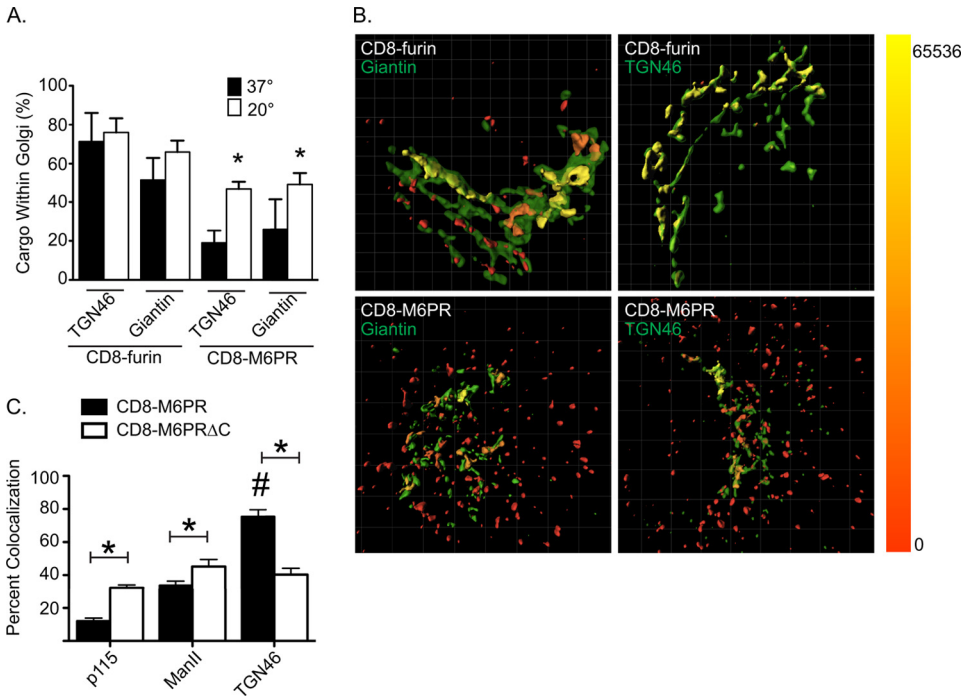

FIGURE 2. **Cargos localize to distinct Golgi compartments and respond to temperature block differently.** HeLaM cells were transiently transfected with plasmids directing the expression of CD8-furin or CD8-M6PR. The next day (~16 h), cells were fixed and labeled for CD8 and TGN46 or giantin. Stacks of images were collected using wide field imaging and were deconvolved, as described under "Experimental Procedures." *A*, deconvolved images were imported into Imaris, and two isosurfaces were defined: one using the cargo (CD8-furin or CD8-M6PR) and the other using a TGN or Golgi marker (TGN46 or giantin). Total cargo fluorescence was calculated for each cell, and then the amount of cargo fluorescence within the Golgi marker isosurface was determined. The values shown indicate the percent of total cargo intensity found within the Golgi marker isosurface, and *bars* indicate S.E. ($n = 5$). Student's *t* test was used to compare 37 °C to 20 °C for each cargo/Golgi marker pairing. *Asterisks* indicate $p < 0.01$. Results are typical of at least three experiments. *B*, isosurfaces were generated for the indicated cargo and markers, as described under "Experimental Procedures." The cargo was falsely colored with a heat map indicating the amount of Golgi marker found within the cargo isosurface. The color range of intensities is shown as a *bar on the right*. *C*, cells expressing either CD8-M6PR or CD8-M6PRΔC were fixed and stained for CD8 and the indicated Golgi marker. Single-plane, confocal images were collected, and the amount of Golgi marker signal that is also positive for cargo was calculated using Mander's coefficients. A Student's *t* test was used to compare the overlap of each cargo with the Golgi marker indicated. An *asterisk* indicates statistical significance ($p < 0.01$).

toward the later Golgi compartments/TGN. Note that the two different methods of quantifying co-localization of two antigens yield very different percentages; *e.g.* ~20% for CD8-M6PR within TGN46 isosurfaces and ~80% for CD8-M6PR and TGN46 using Mander's coefficients. We believe that the 3D3I method yields a much better indication of the location of the antigen within the cell, whereas the latter gives useful information regarding the presence or absence of the antigen within an organelle but can give a false impression of the overall distribution.

When we compared the distribution of CD8-M6PR to that of CD8-M6PRΔC we found statistically significant differences. The amount of CD8-M6PRΔC that overlapped with the markers of early, middle, and late Golgi were all quite similar: p115, 32.3 ± 1.8%; mannosidase II 45.2 ± 4.2%; TGN46 staining 40.2 ± 3.8%. Thus, the truncation of the C terminus resulted in the inability to concentrate within the later compartments of the Golgi, as seen for the full-length CD8-M6PR.

CD8-M6PR Accumulates at the Golgi in Response to a 20 °C Block—To test one aspect of our model, that cargo concentration is a determinant of adaptor recruitment, we sought a minimally invasive method for modulating cargo concentration at a functionally important site in anterograde traffic. We used the previously characterized 20 °C block in which cells are grown at 20 °C for 4 h during which time protein synthesis and export from the ER continue but export from the late Golgi/TGN is inhibited (35, 52–54). Because M6PR acts to escort lysosomal hydrolases and other mannose 6-phosphate modified proteins to lysosomes, its traffic between the Golgi and the endosomal-lysosomal pathway is bi-directional. Thus, a block in protein export from the Golgi in response to the 20 °C block is predicted to cause accumulation of M6PR at the Golgi. To confirm this, CD8-M6PR was expressed in HeLaM cells, and the next day cells were either maintained at 37 °C or incubated at 20 °C for 4 h before fixation. Visual inspection of CD8-M6PR staining confirmed that the cargo is increased at the Golgi during 20 °C block, as evidenced by the increased perinuclear and decreased peripheral staining. To quantify this we used 3D3I to compare the percentage of CD8-M6PR staining that was seen within the isosurface defined by giantin staining and found double the amount; 25.9 ± 15.4% at 37 °C to 49.0 ± 6.2% after the 20 °C block (Fig. 2*A*). Similar results were obtained using cells stably transfected with CD8-M6PR (data not shown).

To determine whether the 20 °C block resulted in changes in intra-Golgi localization of CD8-M6PR, we compared its co-localization with markers of early (p115), medial (giantin), or late (TGN46) Golgi in cells maintained at 37 °C to those after 20 °C block. Although the levels of CD8-M6PR co-localization with each marker were increased, they were increased about equally across these three compartments (data not shown). Thus, we conclude that the absolute amount of CD8-M6PR within compartments of the Golgi was increased during the 20 °C block,

but its distribution within the Golgi as a whole was maintained, with a clear bias toward later compartments.

When we looked at the effects of the temperature block on CD8-M6PRΔC we saw clear increases in cargo in all compartments of the Golgi relative to controls (37 °C) and, again, with no change in its distribution, which in this case was more uniform across Golgi compartments. Cells stably transfected with CD8-M6PRΔC showed similar, uniform distribution throughout the Golgi. Thus, 20 °C block causes both M6PR-based cargos to accumulate in the Golgi, and the cargos retain the same distribution across the Golgi seen in control cells.

Localization of full-length GFP-M6PR in response to temperature block was also tested. HeLaM cells transfected with GFP-M6PR were maintained at 37 °C or temperature blocked for 4 h. Cells were stained with antibodies against GFP and GM130. In cells maintained at 37 °C, GFP-M6PR staining localized predominantly to punctate, endosomal-like structures throughout the cytosol (Fig. 1*C*). After a 20 °C block, GFP-M6PR staining localized prominently in the perinuclear region, overlapping with GM130 staining (data not shown). Thus, the full-length cargo, GFP-M6PR, behaves similarly to the CD8-M6PR, as it is sensitive to temperature block and re-localizes to the Golgi during incubation at 20 °C.

Cargos Are Present in Locations without Adaptors—Because we hope to develop models for cargo-dependent adaptor recruitment, we further investigated the site of adaptor concentration relative to both the cargo and different compartments of the Golgi. We first asked where AP-1 is found in response to cargo expression. The expression of CD8-furin, CD8-M6PR, or CD8-M6PRΔC resulted in increased AP-1 staining in the perinuclear region when compared with mock-transfected cells. We found that there was virtually no recruitment of AP-1 to early Golgi compartments in control cells or those expressing CD8-furin or either CD8-M6PR construct. The amount of AP-1 staining in p115-defined isosurfaces was so small that we did not quantify it. Instead, we compared cargo-dependent concentration of AP-1 to giantin and TGN46 compartments and found a strong bias of AP-1 to these compartments for both CD8-furin and CD8-M6PR at steady state (Fig. 3*A*, *black bars*). As expected, the full cytoplasmic tail of M6PR or that portion that contains the AP-1 binding site each promotes localization of AP-1 to the Golgi. Thus, despite the presence of each of these cargos at early compartments within the Golgi, they are each capable of promoting the binding of AP-1 to only late Golgi compartments. Thus, at steady state the cargos used herein vary in relative abundances at different sites along the endomembrane system but promote the recruitment of adaptors to more spatially restricted sites. We conclude that cargo is necessary but not sufficient for adaptor recruitment and that another factor(s) is required to spatially restrict coat recruitment.

Adaptors Are Lost from M6PR Isosurfaces in Response to 20 °C Block—We predicted that the significant accumulation of CD8-M6PR at the Golgi during the 20 °C block would be matched by increases in both AP-1 and GGA recruitment, as each has been proposed to function in export of M6PRs from that site (24, 55). Furthermore, we predicted that both cargo and adaptors would diminish in abundance during the recovery from the 20 °C block, as carriers containing CD8-M6PR/adaptor pairs exited the Golgi and returned to steady state levels. Unexpectedly, we found that in cells expressing CD8-M6PR the staining of AP-1 (Fig. 3*B*) and GGA1 (Fig. 3*C*) was dramatically reduced during the 20 °C block to the extent that they were indistinguishable from control cells that do not express CD8-M6PR. Similarly, in cells expressing CD8-M6PRΔC, AP-1 staining was significantly decreased (Fig. 3*E*). We also evaluated adaptor recruitment in cells stably transfected with CD8-M6PR or CD8-M6PRΔC and found AP-1 recruitment to be lost after temperature block, recapitulating our observations using transiently transfected cells. The amount of AP-1 recruited to cargo volumes was quantified using 3D3I (Fig. 3*G*). Values were normalized to sum AP-1 intensity/cargo volume and analyzed by Student's *t* test, comparing 37 °C to 20 °C block for each cargo. The decrease in AP-1 staining intensity was significant for both CD8-M6PR and CD8-M6PRΔC, with the latter being more dramatic as a result of the increase in AP-1 staining seen over that with CD8-M6PR in cells maintained at 37 °C.

We also evaluated AP-1 at the Golgi (giantin isosurfaces) in cells expressing CD8-M6PR, CD8-M6PRΔC, or CD8-furin (Fig. 3*H*, quantified in Fig. 3*A*). Consistent with previous results, AP-1 staining at the Golgi is dramatically lowered in response to 20 °C block in cells expressing CD8-M6PR or CD8-M6PRΔC. We also quantified GGA1 staining in cells stably or transiently expressing CD8-M6PR or CD8-M6PRΔC and found that temperature block had the same effect as it did on AP-1, causing its dissociation (Fig. 3*I* and data no shown). Thus, for CD8-M6PR the cargo and adaptors respond in opposite ways to the temperature block, with the cargo being significantly increased in abundance at the Golgi but AP-1 and GGA1 adaptors that presumably facilitate its export from that compartment being lost. These results also support the conclusion that cargo is necessary but not sufficient to recruit adaptors and confirm that additional factors regulate cargo-dependent Arf activation.

We used FAPP2 staining as a control for the effects of the 20 °C block on a cargo-independent, Arf-dependent effector at the Golgi and for general integrity of the Golgi. FAPP2 staining in control HeLaM cells (Fig. 3*D*) or cells over-expressing cargos (data not show) displayed a Golgi pattern of FAPP2 staining that was unchanged by 20 °C block. This provides indirect evidence that neither phosphatidylinositol 4-phosphate levels, required for FAPP2 binding to Golgi (7, 56), nor the "nonspecific" levels of activated Arfs were grossly altered at the Golgi in response to cargo overexpression or temperature block. Our results are consistent with 20 °C block causing only minimal perturbation to Golgi physiology and morphology, as previously reported using related assays (36). In addition we have used mock transfections or homologous cargos, *e.g.* CD8 fused to the cytoplasmic tail of the amyloid precursor protein (CD8-APP) that do not bind AP-1 or GGAs, and found no significant changes in AP-1 (data not shown) or GGA1 recruitment at steady state or after temperature block (Fig. 3*I*). Together, our data show that CD8-M6PR and CD8-M6PRΔC are maintained or increased in abundance at the Golgi in response to 20 °C block but that AP-1 was lost from CD8-M6PR and CD8-M6PRΔC when these proteins were arrested in traffic by a 20 °C block.

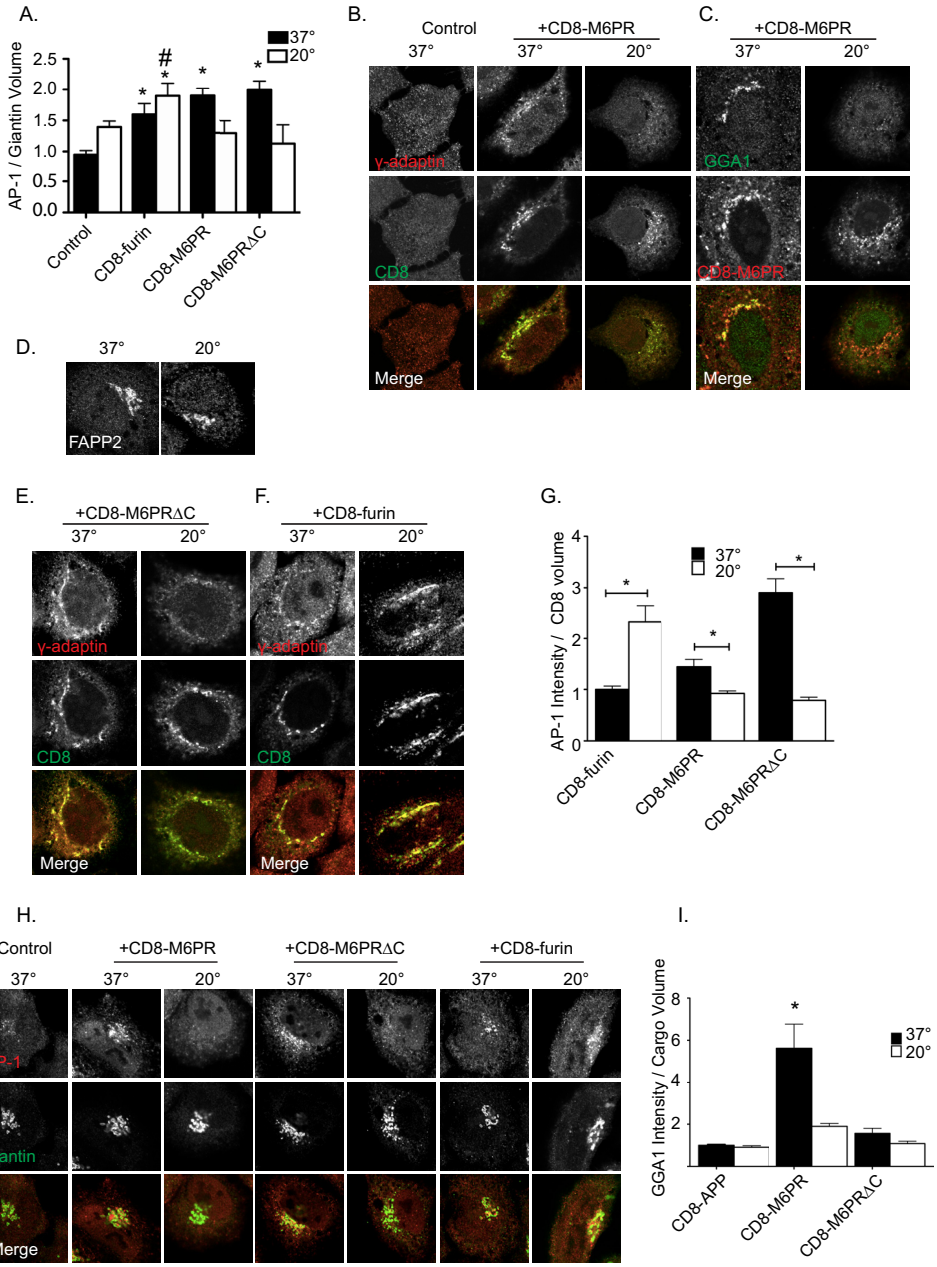

FIGURE 3. **Adaptor recruitment to cargo and Golgi following 20 °C block.** *A*, shown is quantification of AP-1 recruitment to giantin-defined isosurfaces in response to the presence of the indicated cargo. HeLaM cells were transfected with empty vector (*Control*) or those directing expression of the indicated cargos. Eighteen hours later they were placed at 37 °C or 20 °C for 4 h, fixed, and stained with antibodies against AP-1 and giantin. Wide field images were used to generate an isosurface based on cargo staining, and the sum intensity of AP-1 staining within that isosurface was determined. *Bars* represent the mean ratio of AP-1 intensity within the cargo volume. Student's *t* test was used to statistically compare cells at 37 °C and 20 °C for each cargo. *Asterisks* indicate statistical significance differences between cells at different temperatures ($p < 0.01$). # indicates statistical significance between CD8-furin-expressing cells incubated at 37 °C and 20 °C ($p < 0.05$). AP-1 (*B*, *E*, and *F*) or GGA1 (*C*) recruitment in response to cargo expression and temperature block is shown in confocal images. Cells were transfected with the indicated cargos and treated as described above. Cells were stained with antibodies against γ-adaptin and CD8 (*B*, *E*, and *F*) or GGA1 and CD8 (*C*). *D*, HeLaM cells were maintained at 37 °C or 20 °C for 4 h, fixed, and stained for FAPP2. *G*, shown is quantification of AP-1 recruitment to cargo-defined isosurfaces. Wide field images were used to generate an isosurface based on cargo staining, and the sum intensity of AP-1 staining within that isosurface was determined. *Bars* represent the mean ratio of AP-1 intensity within the cargo volume. Student's *t* test was used to statistically compare cells at 37 °C and 20 °C for each cargo. *Asterisks* indicate statistical significance differences in sum intensity of AP-1 within cargo isosurfaces ($p < 0.01$). *H*, AP-1 recruitment to Golgi in cells expressing various cargos, at 37 °C and 20 °C. Cells were prepared and treated as described in *A*. Confocal images are shown. AP-1 recruitment was lost in response to 20 °C block in cells expressing CD8-M6PR and CD8-M6PRΔC but not CD8-furin. *I*, quantification of GGA1 recruitment to cargo volumes is shown. HeLaM cells were transfected with the indicated cargos treated as described above and stained with antibodies against GGA1 and CD8. Images were prepared as described above, and isosurfaces were generated based on CD8 staining. Sum intensity of GGA1 staining within each cargo isosurface is reported. Values are normalized to GGA1 intensity within CD8-APP-defined isosurfaces at 37 °C. Groups were analyzed using analysis of variance, $n > 5$ cells for each condition. *Error bars* indicate S.E., and *asterisks* indicate statistical significance ($p < 0.01$).

Similar results were obtained when GFP-M6PR was expressed in HeLaM cells. GFP-M6PR expression resulted in the recruitment of AP-1 to the perinuclear region at steady state, but this recruitment was lost after temperature block (data not shown).

CD8-furin Shows Little Change in Localization, but AP-1 Recruitment Was Increased in Response to a 20 °C Block—The furin endoprotease acts at the Golgi and is retained there through a mechanism that involves the binding of Mint3 (34). But furin also "escapes" to the endosomal system, using AP-1 in the process (33). Thus, it was difficult to predict what impact the 20 °C block might have on the localization of CD8-furin. The levels of CD8-furin at the Golgi before and after 20 °C block were compared by double staining for CD8-furin and giantin (Fig. 2*A*). The percentages of CD8-furin found within the giantin-defined isosurface before and after 20 °C block were 51.3 ± 11.7 and 66.0 ± 5.8%, respectively (Fig. 2*A*). The percentages of CD8-furin found within TGN46-defined isosurfaces before and after 20 °C block were 71.3 ± 14.8 and 76.0 ± 7.4%, respectively (Fig. 2*A*). The already high fraction of CD8-furin at the Golgi was seen to increase but not significantly ($p > 0.01$). Thus, we found that a 20 °C block is an effective inhibitor of M6PR export from the Golgi/TGN leading to its accumulation there but has a far more limited effect on furin accumulation, likely because furin already accumulates in the Golgi.

In cells expressing FLAG-furin (data not shown), or CD8-furin, AP-1 staining was maintained throughout the 20 °C block (Fig. 3*F*). AP-1 accumulation at CD8-furin-defined isosurfaces was actually significantly increased after 20 °C block compared with cells maintained at 37 °C (Fig. 3*G*). To ensure that the increased recruitment still occurred on Golgi surfaces, we also quantified the AP-1 staining present in giantin isosurfaces in cells with and without 20 °C block (Fig. 3*A*). We found that the 20 °C block increased AP-1 staining into giantin isosurfaces in CD8-furin-expressing cells compared with controls ($p < 0.01$) and rose to the level of statistical significance at the level of $p < 0.05$ (though not $p < 0.01$) when compared with CD8-furin-expressing cells maintained at 37 °C. The CD8-furin-dependent increase in AP-1 is striking at both 37 °C and 20 °C, each significantly higher than controls (Fig. 3*A*) as well as from each other. Thus, the 20 °C block increases the abundance of AP-1 in CD8-furin isosurfaces (Fig. 3*F*) as well as Golgi membranes, defined by giantin staining (Fig. 3*A*). Together with the FAPP2 control, these results highlight the specific and unexpected loss of adaptors from M6PR cargos during temperature block, including both full-length GFP-M6PR and the CD8-M6PR fusion proteins.

BFA Treatment Also Promotes Loss of Adaptors from M6PR, and Recovery Is Initiated at a Site Other than Golgi—We sought an assay independent of temperature changes and more rapid than the 4-h 20 °C block to assess sites of adaptor recruitment. We used the previously characterized ability of BFA to rapidly and reversibly inhibit a subset of Arf GEFs to inhibit Arf activation and Arf-dependent adaptor recruitment in live cells. This provides both a further confirmation that the adaptor recruitment being studied is in fact Arf-dependent and also allows the synchronized re-recruitment of adaptors during recovery from the drug. Treatment with BFA blocks the activation of Arfs

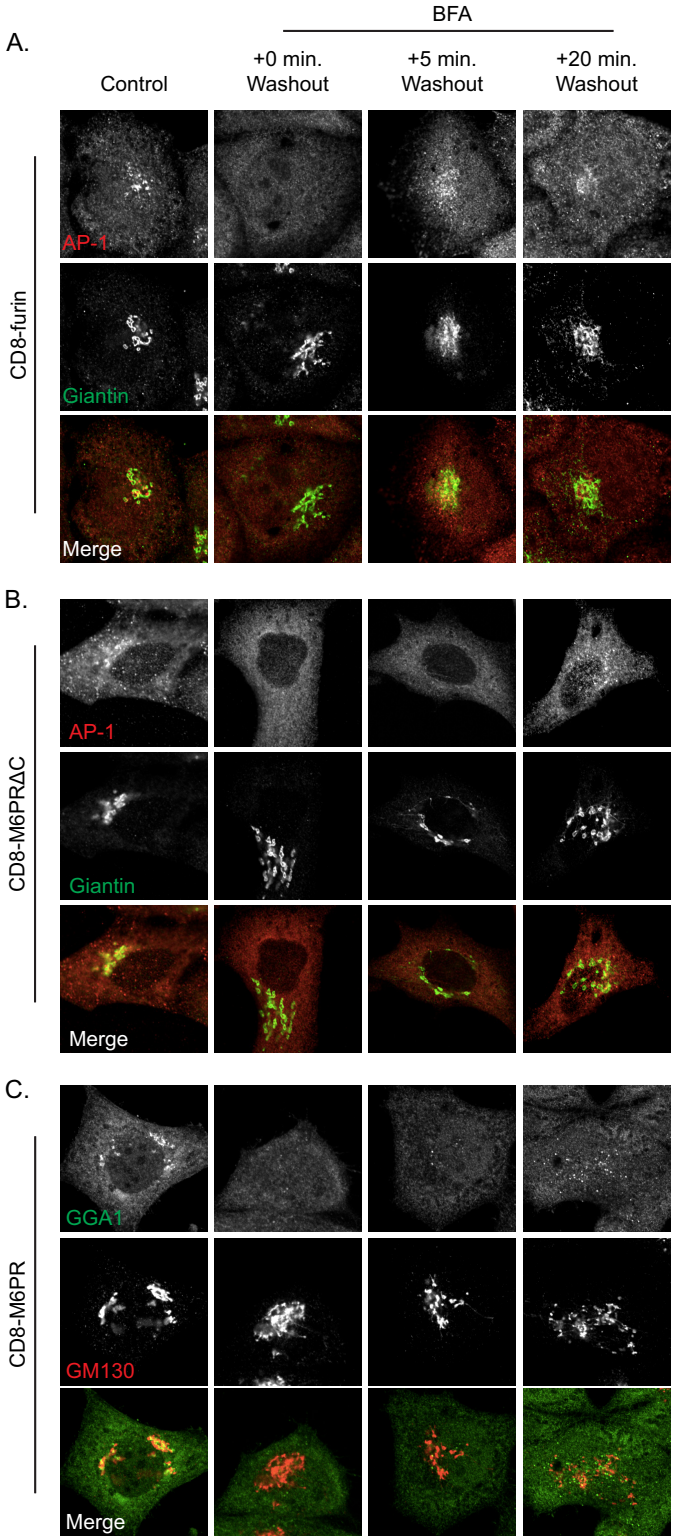

FIGURE 4. **Distinct AP-1 re-recruitment to different cargo during BFA recovery.** HeLaM cells expressing CD8-furin (*A*), CD8-M6PRΔC (*B*), or CD8-M6PR (*C*) were treated with 7.5 μg/ml BFA for 2 min, then the drug was removed, and cells were fixed at the indicated times and stained for AP-1 and giantin (*A* and *B*) or GGA1 and GM130 (*C*). AP-1 recruitment to Golgi membranes is evident within 5 min of BFA washout in CD8-furin-expressing cells. AP-1 (*B*) and GGA1 (*C*) re-recruitment is delayed in cells expressing CD8-M6PRΔC (*B*) or M6PR (*C*) and appears more punctate and peripheral.

within seconds and strips endomembrane structures of Arf-dependent adaptors (40, 57). After a 2-min exposure to BFA (7.5 μg/ml; 0 min recovery) membrane staining of AP-1 (Fig. 4, *A* and *B*), GGA1 (Fig. 4*C*), and Mint3 (data not shown) were completely lost. Only at longer times of BFA treatment (or higher doses) does the Golgi fragment, with retrograde movement of Golgi components to the ER (40). After 2 min of BFA exposure we observed no changes in staining of the Golgi in general (Fig. 4, *A–C*) with the exception that markers of the TGN may become more tubulated in appearance (not evident in the images shown in Fig. 4). And by about 15 min into the recovery phase, staining for Golgi markers typically became less reticular and more globular in appearance.

In CD8-furin-expressing cells, the cargo-dependent recruitment of AP-1 (Fig. 4*A*) and Mint3 (data not shown) were each lost within 2 min of BFA treatment. Within 5 min of BFA washout, both AP-1 (Fig. 4*A*) and Mint3 (data not shown) adaptors were recruited back to the Golgi, returning to control (vehicle only) levels within 10–15 min of washout. The staining of the re-recruited adaptors at each time point was characteristic of Golgi staining; *i.e.* perinuclear, often lamellar in appearance, and showing extensive overlap with giantin. The rapid return of both AP-1 and Mint3 to the Golgi after BFA washout is consistent with that being the initial site of recruitment of each adaptor in response to the presence of CD8-furin. FAPP2 staining was also lost in response to BFA and returned to the Golgi with kinetics indistinguishable from those of adaptors recruited by CD8-furin (data not shown). We conclude that AP-1 and Mint3 are each recruited to the Golgi by CD8-furin in an Arf-dependent, BFA-sensitive manner.

In cells either transiently or stably transfected to express CD8-M6PR, the Golgi re-recruitment of GGA1 and AP-1 after BFA washout was delayed relative to that seen for CD8-furin-dependent adaptors or FAPP2. Also, the pattern of AP-1 and GGA1 staining as they first reappeared differed from that seen in cells that had not been exposed to BFA in that it was more punctate and peripheral. This punctate staining became apparent by ~15 min, whereas the more Golgi-like staining pattern seen in control cells was not evident until ~30 min of recovery from the drug. By 15 min of recovery from BFA, during which time AP-1 had clearly returned to the Golgi/TGN in CD8-furin-expressing cells (Fig. 4*A*), we saw no evidence of Golgi localization of AP-1 in cells expressing CD8-M6PR (data not shown). Similarly, GGA1 was not re-recruited to the Golgi in cells expressing CD8-M6PR (Fig. 4*C*). Thus, the recruitment of both AP-1 and GGA1 in cells expressing CD8-M6PR during recovery from BFA were initiated at a compartment distinct from what was observed for AP-1 and Mint3 recruitment in cells expressing CD8-furin; *i.e.* the Golgi.

In cells expressing CD8-M6PRΔC, the re-recruitment of AP-1 was similar to that seen with CD8-M6PR-expressing cells. AP-1 was recruited to peripheral puncta by about 15 min after washout. By 30 min, AP-1 was localized to Golgi compartments, similar in appearance to cells treated with vehicle only.

BFA treatment and recovery from drugs of cells expressing GFP-M6PR resulted in similar patterns of adaptor recruitment, with BFA treatment causing the loss of both GGA1 and AP-1 staining in the perinuclear region, and only after 15 min washout was recruitment detected. The newly recruited adaptors were again seen first on sites that were clearly distinct from the Golgi as determined by GM130 staining and were identified as recycling endosomes by co-localization with transferrin receptor (TfR).

M6PR Recruits AP-1 and GGA1 Initially to Recycling Endosomes during Recovery from BFA or Temperature Block—As shown in Fig. 4, by 15 min of recovery from BFA there was an indication of return of AP-1 and GGA1 staining to endomembranes in CD8-M6PR-expressing cells but no evident co-localization of adaptors with Golgi markers. To examine the possibility that CD8-M6PR recruits adaptors initially to endosomal compartments, we assessed the re-recruitment of adaptors during recovery from the 20 °C block. As shown in Fig. 5, 20 °C block caused the dissociation of GGA1 and AP-1 (data not shown) from the membranes in cells expressing CD8-M6PR. GGA1 was slowly re-recruited to membranes after shift from 20 °C to 37 °C and was detected on membranes after 15 min of recovery (Fig. 5, *A* and *B*). This amount of time has previously been shown to be sufficient for cargo to exit the Golgi and arrive at a proximal compartment (35). Recovery of AP-1 staining at endomembranes matched that of GGA1 with regard to kinetics and location throughout the recovery. Longer periods of recovery (~30–45 min) resulted in the return to distributions of CD8-M6PR, AP-1, and GGA1 seen in cells that had not undergone temperature block (*i.e.* steady state). Thus, the timing of GGA1 recruitment is consistent with the arrival of CD8-M6PR at a post-Golgi destination.

To identify the compartments to which GGA1 and AP-1 were initially recruited during recovery from the 20 °C block, we co-localized GGA1 in CD8-M6PR-expressing cells with cargo (Fig. 5, *A* and *C*), TfRs (Fig. 5, *B* and *E*), GM130 (Fig. 5*D*), EEA1, Rab11, Lamp I, and Lamp II (data not shown). The strongest co-localization was observed between GGA1 and TfR (Fig. 5*B*) and Rab11 (data not shown), well characterized markers of recycling endosomes (58, 59). Quantification of deconvolved wide field images revealed the loss of GGA1 recruitment to CD8-M6PR after 20 °C block but return of GGA1 staining at CD8-M6PR isosurfaces by about 15 min (Fig. 5*C*). Importantly, we also observed extensive co-localization between GGA1 and TfR isosurfaces by 15 min (Fig. 5*E*). In contrast, there was minimal co-localization between GGA1 and GM130 at that time (Fig. 5*D*).

Because our method of quantifying adaptor recruitment is not widely used yet, we compared results from 3D3I to the more common pixel overlap method of co-localization. Quantification of confocal images using Mander's coefficients was performed with similar results but with larger -fold changes in co-localization. Both methods of quantification reveal a 20 °C block-dependent loss of GGA1 at the Golgi in CD8-M6PR-expressing cells that is not recovering at the Golgi by 15-min release from the block (Fig. 5*D*). Rather, GGA1 recruitment to TfR-positive structures is strongly increased at this time (Fig. 5*E*). AP-1 recruitment profiles and kinetics mimic those of GGA1 in that the adaptors almost completely co-localize and appear at TfR-positive structures at the same time after release from 20 °C block (data not shown). Thus, the CD8-M6PR-dependent recruitment of AP-1 and GGA1 in cells recovering

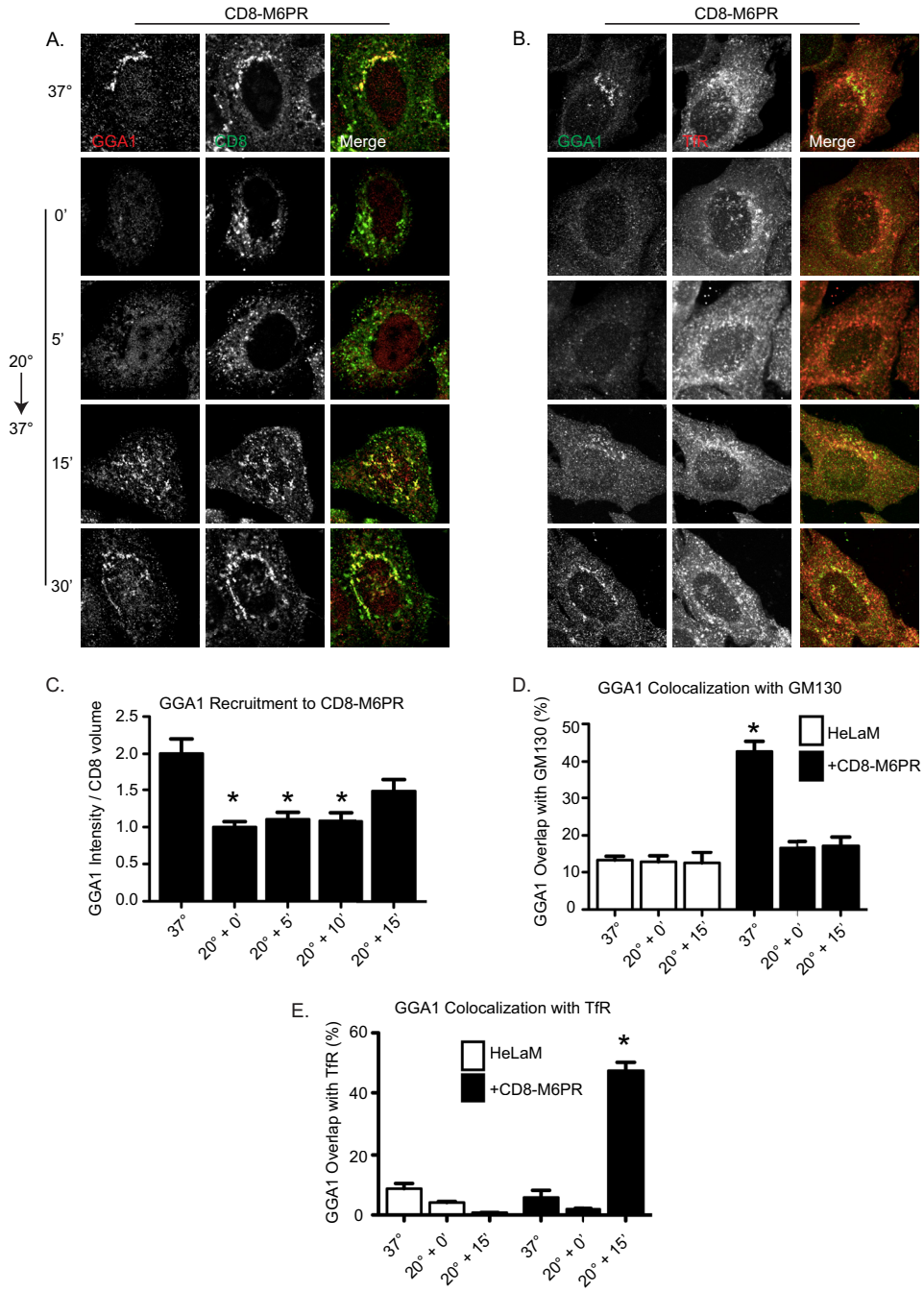

FIGURE 5. **Re-recruitment of adaptors after 20 °C block occurs initially on recycling endosomes in CD8-M6PR-expressing cells.** HeLaM cells expressing CD8-M6PR for 24 h were untreated (37 °C) or temperature-blocked (20 °C) for 4 h before return to 37 °C for the indicated times. Cells were stained for CD8 and GGA1 (*A* and *C*), GGA1 and TfR (*B* and *E*), or GGA1 and GM130 (*D*). CD8-M6PR (*C*) staining was also imaged by wide field microscopy and used to generate isosurfaces into which GGA1 recruitment was quantified and normalized to cells kept at 20 °C for 4 h. GGA1 recruitment to CD8-M6PR was statistically significantly decreased during 20 °C block and returned to control levels only 15 min into recovery. GGA1 intensity within CD8-defined isosurfaces was analyzed using analysis of variance, and *asterisks* indicate $p < 0.01$ compared with steady state ($n > 5$ cell analyzed). *D* and *E*, confocal images were acquired and quantified using M1 and M2 coefficient, as described under "Experimental Procedures." *Bar graphs* represent mean Mander's coefficients of GGA1 intensity that is also GM130-positive (*D*) or GGA1 intensity that is also TfR-positive (*E*). *Error bars* indicate S.E. *Asterisks* indicate $p < 0.01$ when evaluated with a one-way analysis of variance and a Dunnett post-test. All comparisons were made to staining in HeLaM maintained at 37 °C.

from 20 °C block did not occur first at the Golgi, as was seen with CD8-furin, but was primarily at recycling endosomes.

We then asked if the site of recovery of adaptor recruitment observed in cells recovering from 20 °C block agreed or differed from that seen after BFA treatment. Cells expressing CD8-M6PR (Fig. 6), GFP-M6PR, or CD8-M6PRΔC (data not shown) were treated with BFA as in Fig. 5 and double-labeled with antibodies against GGA1 and TfR. GGA1 (Fig. 6) and AP-1 (data not shown) recruitment was seen at ~15 min after washout of BFA and occurred on TfR-positive endosomes. Thus, the site of initial recruitment of GGAs (and AP-1) coincided with the appearance of CD8-M6PR or GFP-M6PR after the release from 20 °C block or BFA and was found in each case to be recycling endosomes and not the Golgi. Adaptor re-recruit-

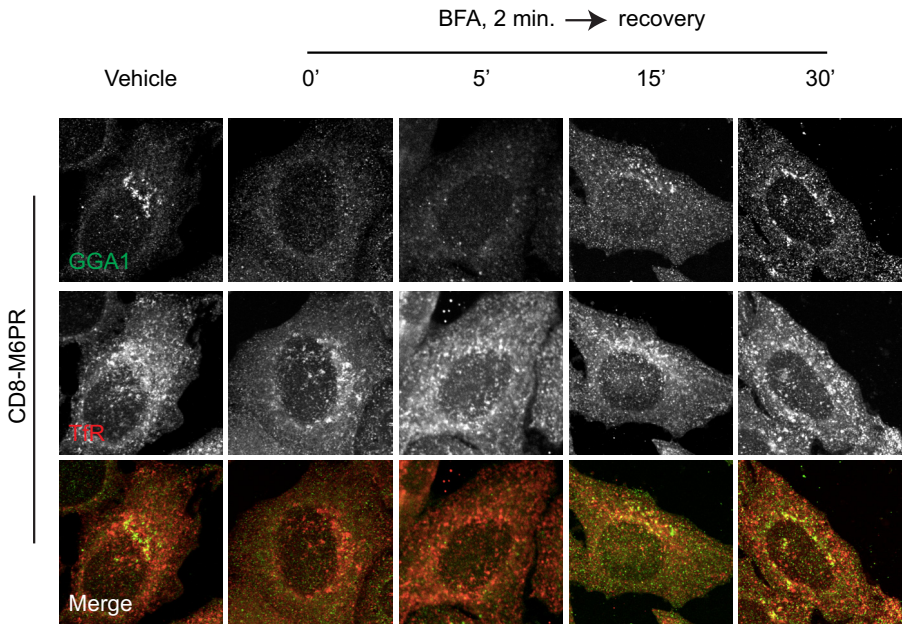

FIGURE 6. **GGA1 recruitment to M6PR is delayed after BFA washout and co-localizes with TfR.** HeLaM cells expressing CD8-M6PR were treated with vehicle (0.175% methanol) or 7.5 μg/ml BFA for 2 min, then BFA was removed, and cells were allowed to recover for the times indicated, fixed, and stained for GGA1 and TfR.

ment to TfR-positive endosomes was observed in both transiently and stably transfected cells. These results also suggest that the 20 °C block did not result in gross, persistent changes to the rate of cargo export either as a result of cargo accumulation or the exposure to lower temperature, as the arrival of new M6PR from the Golgi/TGN to recycling endosomes was about the same for release from 20 °C block and BFA washout. These results are in marked contrast to those obtained with CD8-furin, in which AP-1 was recruited initially to the Golgi after BFA removal (Fig. 4). These results also serve as a control to confirm that the washout was effective and intracellular BFA concentrations were reduced to ineffective levels quickly.

NRK Cell Data—Temperature block (data not shown) and BFA recovery experiments were repeated in NRK cells, the cell type originally used in different laboratories to describe GGA localization at the Golgi (60–62). Control (non-transfected) NRK cells have more GGA1 and AP-1 staining in the perinuclear area than do HeLaM cells, as staining with antibodies at the same concentration resulted in greater intensity signal (compare Figs. 1*A* and 7*A*). Cells were fixed and stained with antibodies against GGA1 and AP-1 (Fig. 7*A*, *upper panels*) or GGA1 and GM130 (Fig. 7*A, lower panels*). Overlap in staining of the two adaptors and of GGA1 with the Golgi marker, GM130, is clearly evident. Although the nature of the endogenous cargo(s) responsible for higher levels of GGA1 and AP-1 staining in NRK cells is unknown, the adaptors behave very similarly (see below) to those recruited by CD8-M6PR or GFP-M6PR in HeLaM cells. We interpret these findings as further evidence that neither protein overexpression nor the fusion proteins used in our studies alter responsiveness of adaptors.

GGA1 and AP-1 staining were each lost in response to the 20 °C block in both control NRK cells (Fig. 7*A*) and those expressing CD8-M6PR (data not shown). As in HeLaM cells, GGA1 and AP-1 recruitment in NRK during recovery from 20 °C block occurred onto structures that appeared quite different from Golgi, beginning ~15 min after release (Fig. 7*A*). We confirmed that these are recycling endosomes based upon extensive overlap with TfR staining (data not shown).

BFA treatment of NRK cells (data not shown) or NRK cells expressing HA-GGA1 resulted in rapid GGA1 dissociation from membranes that failed to re-recruit directly onto Golgi membranes at early times during recovery from the drug (Fig. 7*B*). Rather, both GGA1 and AP-1 were first found on TfR^+ endosomes. Thus, the endogenous cargo(s) in NRK cells responsible for higher steady state levels of AP-1 and GGAs at Golgi membranes, like M6PR, recruit these adaptors initially to recycling endosomes and only later to the Golgi.

DISCUSSION

Arfs and Arf-dependent adaptors regulate cargo traffic and/or retention in the secretory and endocytic pathways. Despite years of research, we still lack clear molecular models for the nature of the signal that leads to Arf activation and adaptor recruitment. Our goal was to define an experimental model to begin dissecting aspects of Arf activation and adaptor recruitment that retain the specificity and biological relevance seen in intact cells. We used fluorescence imaging of HeLaM cells after transient expression of model cargos combined with two independent manipulations, temperature block and BFA treatment, for evaluating the Arf- and cargo-dependent recruitment of adaptors at Golgi and recycling endosomes by monitoring recovery from each treatment. These provided consistent results and strengthen the conclusions drawn from each. Our results demonstrate that the specificities of cargo-adaptor interactions documented using *in vitro* assays are faithfully preserved in cells. We also discovered that the cytoplasmic tail of M6PR recruits both AP-1 and GGAs first to recycling endosomes after recovery from either BFA treatment or cold tem-

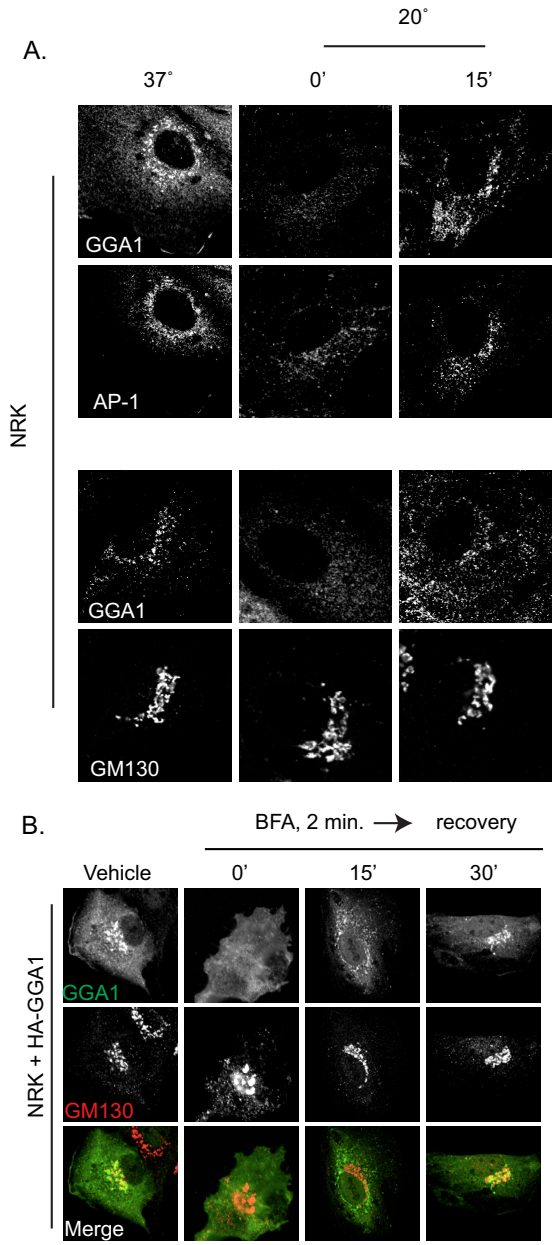

FIGURE 7. **GGAs and AP-1 are lost during temperature block or BFA treatment in NRK cells and return first on endosomes.** *A*, NRK cells were maintained at 37 °C (*left panels*) or subjected to 20 °C temperature block for 4 h (*0′*, *middle panels*) or then recovery for 15 min at 37 °C (*15′*, *right panels*). Fixed cells were stained with antibodies against GGA1 and γ-adaptin (AP-1) (*upper panels*) or GGA1 and GM130 (*lower panels*). As in HeLaM cells expressing CD8 fusions or full-length cargos, GGA1 and AP-1 were lost in response to temperature block, and re-recruitment was delayed after release and occurred on small, peripheral puncta. *B*, NRK cells were transfected with HA-GGA1 and the next day were treated with vehicle or BFA (2 min, 7.5 μg/ml) before washout and recovery for 15 or 30 min. Cells were fixed and stained with antibodies against GGA1 (*top panels*) and GM130 (*middle panels*) or false colored before merging (*bottom panels*). Confocal images are shown.

perature blockade and only later displays a prominent Golgi distribution pattern. That AP-1 and GGAs behaved the same in M6PR-expressing cells is consistent with the proposal that they work together (24), although not necessarily to coordinate the packaging of cargos for export from the Golgi. Because the same results were obtained with CD8-M6PR and GFP-M6PR in HeLaM cells and endogenous proteins in NRK cells, we believe these are generally true of a subset of physiologically important cargos, including M6PR. The initial recruitment of AP-1 to recycling endosomes by M6PR is in clear contrast to its recruitment at the Golgi by CD8-furin. These results point to a clear need to define the roles of the different adaptors by both cargo and location, as there is increasing evidence that adaptors may have the capacity to act at different sites to carry out different and even opposing actions in cells. Finally, the specificity of adaptor recruitment by different cargos is evidence against a model in which activated Arfs are freely available on membrane surfaces. Rather, we conclude that Arfs must remain coupled in some way to the Arf GEF or cargo responsible for their activation. This is predicted but unproven to be a direct, physical coupling.

Our goal was to test the hypothesis that cargo acts upstream of Arf activation, perhaps analogous to the roles of ligands in G protein-coupled receptor- or receptor-tyrosine kinase-mediated activation of G proteins and Ras, respectively. Ras is likely the better analogy as cargos lack Arf GEF activity, whereas G protein-coupled receptors serve that role themselves. Adaptors studied here are Arf-dependent because they have been shown in one or more biochemical assay to bind directly to Arfs in a GTP-sensitive fashion and rapidly dissociate from Golgi membranes upon exposure of cells to BFA, and activated Arfs increase their binding to biological membranes or synthetic liposomes in reconstitution assays (63–66). We believe that adaptor recruitment was confirmed as a legitimate surrogate for Arf activation in our studies as each of the adaptors was Arf-dependent and BFA-sensitive and was recruited in a cargo-dependent fashion to different sites, and adaptor recruitment was only ever observed at locations containing cargo. The role of activated Arfs in the recruitment of adaptors is incompletely understood but is typically modeled as facilitating adaptor-cargo association by direct binding to adaptor and orienting it on the surface of the membrane to promote binding to cargo. The observations that increasing the density of different cargo at endomembranes (through specific overexpression with or without temperature block) resulted in the recruitment of some adaptors, but not others, leads us to propose that the cargos are likely to play a more direct role in adaptor recruitment and Arf activation than previously appreciated. For example, it appears unlikely that activation of an Arf GEF would lead to the generation of Arf-GTP that is diffusible within the two-dimensional space of a membrane and recruit adaptors independently of an associated cargo, as this would predict the recruitment of all Arf-dependent adaptors at that site.

A model for Arf6 acting at sites quite distant from its site of activation has recently been proposed (67), but the actions of Arf6 at the cell surface differ substantially from those of Arfs 1–5 on endomembranes so it is not clear how comparable these studies will prove to be. We currently lack direct evidence of specific cargo-GEF-Arf complex formation and must also consider additional components acting between the cargo and the Arf GEFs. We believe the experimental system developed here will be useful in studies to explore the role of different cargos in facilitating activation of specific Arf GEF, recruitment, and activation of specific Arf isoforms (3), Arf GTPase-activating proteins, and other regulators of carrier biogenesis.

The choice of furin as one of the cargos studied was fortuitous as it shares the ability to bind AP-1 with M6PR, has a short cytoplasmic tail, localizes strongly to the Golgi, and was found to behave as predicted in response to BFA or temperature block, thus serving as a very important control for other cargos. We found that CD8-furin or FLAG-furin localized to the Golgi where it bound AP-1 in a BFA-sensitive manner. We showed that CD8-furin is predominantly found on Golgi membranes at steady state so that there was relatively little enhancement in cargo staining in response to 20 °C block. With only small increases in cargo it was surprising to observe the increase in Golgi staining of AP-1 upon 20 °C block of CD8-furin-expressing cells. One explanation for these results is that during 20 °C block a subset of CD8-furin escapes the retention mechanism and becomes available for export and AP-1 binding but is prevented from export by the 20 °C block. This is consistent with the previously described role of AP-1 in the exit of furin from the Golgi and the idea that this represents a small subset of the cargo that escapes retention mechanisms there. In future studies it may be possible to determine the localization of AP-1 under these conditions by electron microscopy to determine if two pools of CD8-furin may be identified, bound to distinct adaptors and possibly at distinct domains of the Golgi/TGN. Importantly, furin constructs and the AP-1 that was recruited by them behaved in every other respect as predicted in that AP-1 was (i) recruited to the Golgi in response to furin expression, (ii) rapidly lost upon exposure to BFA, (iii) returned directly onto Golgi membranes at the earliest time points during recovery from the drug, and (iv) was retained, even increased, during temperature blockade. Thus, this cargo retained the ability to bind AP-1 throughout the temperature block and recovery. Although we had assumed this would be standard for all cargos, it was not the case for M6PR and led to quite different results. The retention of adaptors in furin-expressing cells and of FAPP2 in all cells subjected to temperature block indicates that the lower temperature likely does not itself change Arf activities.

M6PR traffic is bi-directional, between the Golgi and endosomes/lysosomes, although it can also appear on the cell surface (25, 68, 69). We propose recycling endosomes as the initial site of action of AP-1 and GGA1 in regulating sorting and packaging of M6PRs into carriers, although we cannot predict from our data whether the destination of those carriers is the TGN, plasma membrane, or an alternate organelle. Our conclusion is based upon four observations, (i) the delay in recruitment of AP-1 and GGAs during recovery from temperature block of CD8-M6PR-expressing cells in comparison to CD8-furin or FLAG-furin recruitment of AP-1 to the Golgi, (ii) transient but robust co-localization of GGAs and AP-1 with TfR and Rab11 as the initial site of re-recruitment during recovery from temperature block, (iii) identification of recycling endosomes as the site of initial recruitment of GGAs and AP-1 after washout of BFA, and (iv) demonstration that AP-1 is recruited initially to the Golgi during recovery from either temperature block or BFA exposure in CD8-furin-expressing cells. This last point essentially serves as a control in that it emphasizes the fact that AP-1 can be recruited to the Golgi/TGN in HeLaM cells under the conditions used but that CD8-M6PR fails to do so.

That CD8-M6PR was effectively concentrated at the Golgi/TGN during temperature block was expected, but the observation that the adaptors dissociate in the process was novel and quite surprising. During recovery from temperature block the accumulated CD8-M6PR returns toward levels seen in control cells with kinetics that resemble those of export from the Golgi/TGN. Those rates are consistent with CD8-M6PR leaving the TGN and going directly to recycling endosomes. However, we note that this step did not appear to require the recruitment of detectible AP-1 or GGAs to the Golgi/TGN. A role for AP-1 and GGA1 recruitment to CD8-M6PR at recycling endosomes and not at the Golgi/TGN was further supported by BFA experiments, in which adaptors were recruited initially to CD8-M6PR at recycling endosomes and appeared on Golgi/TGN only later. BFA treatment has been previously shown to cause a redistribution of M6PR resulting in its increased levels at the cell surface, although that study used higher concentrations and longer times of BFA treatment that caused Golgi breakdown and redistribution to the ER (57), neither of which occurred in our study. Thus, it is possible that the increase in AP-1 and GGA1 staining seen first at recycling endosomes after recovery from BFA could result from arrival of CD8-M6PR from the cell surface rather than that exiting the Golgi, although we consider this less likely. And even if true, it does not change our conclusion that AP-1 and GGA1 are recruited initially to recycling endosomes after recovery from BFA.

Early reports of the discovery of GGAs as Arf-dependent adaptors reported recruitment to the Golgi and BFA sensitivity. We have verified our results and those of others (60–62, 70) in finding that steady state staining of GGAs in cells expressing GGA binding cargo appears to overlap more closely with Golgi markers than with endosomal markers. The differences we describe here cannot be ascribed to cell type specificities as we obtained the same results in HeLaM and NRK cells. In a more recent study of GGA and AP-1 localization at both the light and EM level in *Drosophila* Dmel2 and HeLa cells, Hirst *et al.* (71) described cargo-dependent recruitment and discovered that AP-1 and GGA staining are in close apposition, although they are not superimposable. The authors point out the difficulties in clearly discriminating between Golgi and endosomal staining and acknowledge that both AP-1 and GGA staining is equally likely to be endosomal. Thus, we cannot exclude the possibility that at steady state, GGAs are on either membrane or both. This striking difference with results of our co-localization of GGA1 or AP-1 with recycling endosome markers may be explained by the transient nature of this initial recruitment that was only revealed in our protocols that led to the removal of previously bound adaptors and allowed a focus on the pool of newly recruited adaptors in CD8-M6PR-expressing cells.

Another formal possibility for the apparent differences in GGA recruitment in steady state cells and those recovering from 20 °C block or BFA treatments is that steady state staining of adaptors may not represent predominantly those involved in carrier biogenesis. If adaptors are retained on mature carriers and the process of uncoating at their desti-

nation is slower than that of coating at their source, then the steady state staining could give an erroneous impression of the site of adaptor recruitment. Recent reports of complexes involved in tethering of carriers at destination organelles are consistent with our suggestion that vesicle fusion may be the rate-limiting step in movement of a carrier from one site to another (*e.g.* see Cai *et al.* (72)). Of course, the observation that CD8-M6PR recruits AP-1 and GGAs first to recycling endosomes in no way challenges the conclusion that each of these adaptors may also be recruited to the TGN, or other sites, by other cargos. Indeed, we showed that CD8-furin recruits AP-1 initially to the Golgi.

We find a number of findings in the literature that further support our conclusion that AP-1 and GGAs are recruited initially to recycling endosomes in response to the presence of CD8-M6PR or M6PR itself. AP-1 has been reported previously to bind endosomes and to function in the retrograde traffic of cargos from endosomes to the TGN (73–76), including that of the M6PRs. There is also evidence that GGA3 can be recruited to recycling endosomes (77) and even by the tail of M6PR (78). These earlier reports suggest specificity for GGA3, but we observed an almost complete pairing of AP-1 recruitment and all three GGAs in CD8-M6PR expressing HeLaM cells. Even the earliest reports of GGA localization included suggestions of binding to or actions at endosomes (61, 62). GGAs, but more specifically GGA3, also have been reported to be recruited to endosomes by BACE1 (77, 79, 80). Interestingly, He *et al.* (79) also compare BACE1 localization to that of a BACE1 fusion protein that swaps out the cytoplasmic tail of the CD8-M6PR and found striking similarities. Depletion of GGAs or expression of a BACE1 mutant that cannot bind GGAs resulted in accumulation of BACE1 at endosomes, leading those authors to propose roles for GGA in both directions of TGN-endosome BACE1 traffic. We speculate that more cargos will be found to recruit GGAs, alone or in parallel with AP-1, to endosomes although we emphasize that simply demonstrating that a particular adaptor binds to a cargo can no longer be taken as evidence for its role at a particular site. Together, our findings demonstrate that the recruitment of the adaptors to regulate carrier biogenesis is cargo-dependent and that adaptors are not limited to a single site of action.

There is currently no molecular model to explain why one cargo-adaptor pair is retained during temperature block (CD8-furin or FLAG-furin with AP-1) and another is lost (CD8-M6PR or GFP-M6PR with AP-1 or GGA1). This behavior and others, including differences in localization within the Golgi of CD8-M6PR and CD8-M6PRΔC, argue strongly for the existence of additional steps in the regulation or "activation" of cargo that leads to downstream actions that include Arf GEF activation. Such regulation likely includes phosphorylation of cargo tail or adaptor (81–83), other post-translational modifications, changes in lipid composition, or binding of regulatory components. We believe that dissection of these complex processes and the spatially and temporally controlled changes involved will require the integration of biochemical, high resolution structural, and cell-based studies and that the cell-based models developed herein will allow these questions to be addressed in the near future.

Acknowledgments—We thank Melanie Styers and Victor Faundez for assistance in editing earlier versions of the manuscript and providing critical feedback. We gratefully acknowledge Gary Thomas (Oregon Health and Science University) and Margaret Robinson and Matthew Seaman (University of Cambridge) for sharing plasmids and/or cell lines and Antonella De Matteis for the generous gift of the FAPP2 antibody.

REFERENCES

1. Kuge, O., Dascher, C., Orci, L., Rowe, T., Amherdt, M., Plutner, H., Ravazzola, M., Tanigawa, G., Rothman, J. E., and Balch, W. E. (1994) Sar1 promotes vesicle budding from the endoplasmic reticulum but not Golgi compartments. *J. Cell Biol.* **125,** 51–65
2. Nakaño, A., and Muramatsu, M. (1989) A novel GTP-binding protein, Sar1p, is involved in transport from the endoplasmic reticulum to the Golgi apparatus. *J. Cell Biol.* **109,** 2677–2691
3. Volpicelli-Daley, L. A., Li, Y., Zhang, C. J., and Kahn, R. A. (2005) Isoform-selective effects of the depletion of ADP-ribosylation factors 1–5 on membrane traffic. *Mol. Biol. Cell* **16,** 4495–4508
4. Bonifacino, J. S., and Traub, L. M. (2003) Signals for sorting of transmembrane proteins to endosomes and lysosomes. *Annu. Rev. Biochem* **72,** 395–447
5. Aridor, M., and Traub, L. M. (2002) Cargo selection in vesicular transport. The making and breaking of a coat. *Traffic* **3,** 537–546
6. Cockcroft, S., Thomas, G. M., Fensome, A., Geny, B., Cunningham, E., Gout, I., Hiles, I., Totty, N. F., Truong, O., and Hsuan, J. J. (1994) Phospholipase D. a downstream effector of ARF in granulocytes. *Science* **263,** 523–526
7. Godi, A., Pertile, P., Meyers, R., Marra, P., Di Tullio, G., Iurisci, C., Luini, A., Corda, D., and De Matteis, M. A. (1999) ARF mediates recruitment of PtdIns-4-OH kinase-β and stimulates synthesis of PtdIns(4,5)P2 on the Golgi complex. *Nat. Cell Biol.* **1,** 280–287
8. Jones, D. H., Morris, J. B., Morgan, C. P., Kondo, H., Irvine, R. F., and Cockcroft, S. (2000) Type I phosphatidylinositol 4-phosphate 5-kinase directly interacts with ADP-ribosylation factor 1 and is responsible for phosphatidylinositol 4,5-bisphosphate synthesis in the golgi compartment. *J. Biol. Chem.* **275,** 13962–13966
9. Margolis, B., and Skolnik, E. Y. (1994) Activation of Ras by receptor tyrosine kinases. *J. Am. Soc. Nephrol.* **5,** 1288–1299
10. Robinson, M. S., and Bonifacino, J. S. (2001) Adaptor-related proteins. *Curr. Opin. Cell Biol.* **13,** 444–453
11. Rothman, J. E., and Orci, L. (1992) Molecular dissection of the secretory pathway. *Nature* **355,** 409–415
12. Rothman, J. E., and Wieland, F. T. (1996) Protein sorting by transport vesicles. *Science* **272,** 227–234
13. Lee, M. C., Miller, E. A., Goldberg, J., Orci, L., and Schekman, R. (2004) Bi-directional protein transport between the ER and Golgi. *Annu. Rev. Cell Dev. Biol.* **20,** 87–123
14. Letourneur, F., Gaynor, E. C., Hennecke, S., Démollière, C., Duden, R., Emr, S. D., Riezman, H., and Cosson, P. (1994) Coatomer is essential for retrieval of dilysine-tagged proteins to the endoplasmic reticulum. *Cell* **79,** 1199–1207
15. Cosson, P., and Letourneur, F. (1994) Coatomer interaction with di-lysine endoplasmic reticulum retention motifs. *Science* **263,** 1629–1631
16. Sohn, K., Orci, L., Ravazzola, M., Amherdt, M., Bremser, M., Lottspeich, F., Fiedler, K., Helms, J. B., and Wieland, F. T. (1996) A major transmembrane protein of Golgi-derived COPI-coated vesicles involved in coatomer binding. *J. Cell Biol.* **135,** 1239–1248
17. Fiedler, K., Veit, M., Stamnes, M. A., and Rothman, J. E. (1996) Bimodal interaction of coatomer with the p24 family of putative cargo receptors. *Science* **273,** 1396–1399
18. Jacobsen, L., Madsen, P., Nielsen, M. S., Geraerts, W. P., Gliemann, J.,

Smit, A. B., and Petersen, C. M. (2002) The sorLA cytoplasmic domain interacts with GGA1 and -2 and defines minimum requirements for GGA binding. *FEBS Lett.* **511,** 155–158
19. Borg, J. P., Ooi, J., Levy, E., and Margolis, B. (1996) The phosphotyrosine interaction domains of X11 and FE65 bind to distinct sites on the YENPTY motif of amyloid precursor protein. *Mol. Cell. Biol.* **16,** 6229–6241
20. Owen, D. J., and Evans, P. R. (1998) A structural explanation for the recognition of tyrosine-based endocytotic signals. *Science* **282,** 1327–1332
21. Aguilar, R. C., Ohno, H., Roche, K. W., and Bonifacino, J. S. (1997) Functional domain mapping of the clathrin-associated adaptor medium chains μ1 and μ2. *J. Biol. Chem.* **272,** 27160–27166
22. Liu, Y., Kahn, R. A., and Prestegard, J. H. (2010) Dynamic structure of membrane-anchored Arf·GTP. *Nat. Struct. Mol. Biol.* **17,** 876–881
23. Jian, X., Cavenagh, M., Gruschus, J. M., Randazzo, P. A., and Kahn, R. A. (2010) Modifications to the C terminus of Arf1 alter cell functions and protein interactions. *Traffic* **11,** 732–742
24. Doray, B., Ghosh, P., Griffith, J., Geuze, H. J., and Kornfeld, S. (2002) Cooperation of GGAs and AP-1 in packaging MPRs at the trans-Golgi network. *Science* **297,** 1700–1703
25. Puertollano, R., Aguilar, R. C., Gorshkova, I., Crouch, R. J., and Bonifacino, J. S. (2001) Sorting of mannose 6-phosphate receptors mediated by the GGAs. *Science* **292,** 1712–1716
26. Klumperman, J., Kuliawat, R., Griffith, J. M., Geuze, H. J., and Arvan, P. (1998) Mannose 6-phosphate receptors are sorted from immature secretory granules via adaptor protein AP-1, clathrin, and syntaxin 6-positive vesicles. *J. Cell Biol.* **141,** 359–371
27. Karlsson, K., and Carlsson, S. R. (1998) Sorting of lysosomal membrane glycoproteins lamp-1 and lamp-2 into vesicles distinct from mannose 6-phosphate receptor/γ-adaptin vesicles at the trans-Golgi network. *J. Biol. Chem.* **273,** 18966–18973
28. Geuze, H. J., Stoorvogel, W., Strous, G. J., Slot, J. W., Bleekemolen, J. E., and Mellman, I. (1988) Sorting of mannose 6-phosphate receptors and lysosomal membrane proteins in endocytic vesicles. *J. Cell Biol.* **107,** 2491–2501
29. Arighi, C. N., Hartnell, L. M., Aguilar, R. C., Haft, C. R., and Bonifacino, J. S. (2004) Role of the mammalian retromer in sorting of the cation-independent mannose 6-phosphate receptor. *J. Cell Biol.* **165,** 123–133
30. Tikkanen, R., Obermüller, S., Denzer, K., Pungitore, R., Geuze, H. J., von Figura, K., and Höning, S. (2000) The dileucine motif within the tail of MPR46 is required for sorting of the receptor in endosomes. *Traffic* **1,** 631–640
31. Hirst, J., Seaman, M. N., Buschow, S. I., and Robinson, M. S. (2007) The role of cargo proteins in GGA recruitment. *Traffic* **8,** 594–604
32. Thomas, G. (2002) Furin at the cutting edge. from protein traffic to embryogenesis and disease. *Nat. Rev. Mol. Cell Biol.* **3,** 753–766
33. Teuchert, M., Schäfer, W., Berghöfer, S., Hoflack, B., Klenk, H. D., and Garten, W. (1999) Sorting of furin at the trans-Golgi network. Interaction of the cytoplasmic tail sorting signals with AP-1 Golgi-specific assembly proteins. *J. Biol. Chem.* **274,** 8199–8207
34. Han, J., Wang, Y., Wang, S., and Chi, C. (2008) Interaction of Mint3 with furin regulates the localization of furin in the trans-Golgi network. *J. Cell Sci.* **121,** 2217–2223
35. Griffiths, G., Pfeiffer, S., Simons, K., and Matlin, K. (1985) Exit of newly synthesized membrane proteins from the trans cisterna of the Golgi complex to the plasma membrane. *J. Cell Biol.* **101,** 949–964
36. Ladinsky, M. S., Wu, C. C., McIntosh, S., McIntosh, J. R., and Howell, K. E. (2002) Structure of the Golgi and distribution of reporter molecules at 20 °C reveals the complexity of the exit compartments. *Mol. Biol. Cell* **13,** 2810–2825
37. Matlin, K. S., and Simons, K. (1983) Reduced temperature prevents transfer of a membrane glycoprotein to the cell surface but does not prevent terminal glycosylation. *Cell* **34,** 233–243
38. Saraste, J., Palade, G. E., and Farquhar, M. G. (1986) Temperature-sensitive steps in the transport of secretory proteins through the Golgi complex in exocrine pancreatic cells. *Proc. Natl. Acad. Sci. U.S.A.* **83,** 6425–6429
39. Donaldson, J. G., Lippincott-Schwartz, J., Bloom, G. S., Kreis, T. E., and Klausner, R. D. (1990) Dissociation of a 110-kDa peripheral membrane protein from the Golgi apparatus is an early event in brefeldin A action. *J. Cell Biol.* **111,** 2295–2306
40. Lippincott-Schwartz, J., Yuan, L. C., Bonifacino, J. S., and Klausner, R. D. (1989) Rapid redistribution of Golgi proteins into the ER in cells treated with brefeldin A. Evidence for membrane cycling from Golgi to ER. *Cell* **56,** 801–813
41. Traub, L. M., Ostrom, J. A., and Kornfeld, S. (1993) Biochemical dissection of AP-1 recruitment onto Golgi membranes. *J. Cell Biol.* **123,** 561–573
42. Molloy, S. S., Thomas, L., VanSlyke, J. K., Stenberg, P. E., and Thomas, G. (1994) Intracellular trafficking and activation of the furin proprotein convertase. Localization to the TGN and recycling from the cell surface. *EMBO J.* **13,** 18–33
43. Valnes, K., and Brandtzaeg, P. (1985) Retardation of immunofluorescence fading during microscopy. *J. Histochem. Cytochem.* **33,** 755–761
44. Bolte, S., and Cordelières, F. P. (2006) A guided tour into subcellular colocalization analysis in light microscopy. *J. Microsc.* **224,** 213–232
45. North, A. J. (2006) Seeing is believing? A beginners guide to practical pitfalls in image acquisition. *J. Cell Biol.* **172,** 9–18
46. Caster, A. H., and Kahn, R. A. (2012) Computational method for calculating fluorescence intensities within three-dimensional structures in cells. *Cell. Logist.* **2,** 176–188
47. Seaman, M. N. (2007) Identification of a novel conserved sorting motif required for retromer-mediated endosome-to-TGN retrieval. *J. Cell Sci.* **120,** 2378–2389
48. Seaman, M. N. (2004) Cargo-selective endosomal sorting for retrieval to the Golgi requires retromer. *J. Cell Biol.* **165,** 111–122
49. Takatsu, H., Katoh, Y., Shiba, Y., and Nakayama, K. (2001) Golgi-localizing, γ-adaptin ear homology domain, ADP-ribosylation factor-binding (GGA) proteins interact with acidic dileucine sequences within the cytoplasmic domains of sorting receptors through their Vps27p/Hrs/STAM (VHS) domains. *J. Biol. Chem.* **276,** 28541–28545
50. Höning, S., Griffith, J., Geuze, H. J., and Hunziker, W. (1996) The tyrosine-based lysosomal targeting signal in lamp-1 mediates sorting into Golgi-derived clathrin-coated vesicles. *EMBO J.* **15,** 5230–5239
51. Heilker, R., Manning-Krieg, U., Zuber, J. F., and Spiess, M. (1996) *In vitro* binding of clathrin adaptors to sorting signals correlates with endocytosis and basolateral sorting. *EMBO J.* **15,** 2893–2899
52. Saraste, J., and Kuismanen, E. (1984) Pre- and post-Golgi vacuoles operate in the transport of Semliki Forest virus membrane glycoproteins to the cell surface. *Cell* **38,** 535–549
53. Mottet, G., Tuffereau, C., and Roux, L. (1986) Reduced temperature can block different glycoproteins at different steps during transport to the plasma membrane. *J. Gen. Virol.* **67,** 2029–2035
54. Lodish, H. F., and Kong, N. (1983) Reversible block in intracellular transport and budding of mutant vesicular stomatitis virus glycoproteins. *Virology* **125,** 335–348
55. Ghosh, P., and Kornfeld, S. (2004) The cytoplasmic tail of the cation-independent mannose 6-phosphate receptor contains four binding sites for AP-1. *Arch Biochem. Biophys.* **426,** 225–230
56. Godi, A., Di Campli, A., Konstantakopoulos, A., Di Tullio, G., Alessi, D. R., Kular, G. S., Daniele, T., Marra, P., Lucocq, J. M., De Matteis, M. A. (2004) FAPPs control Golgi-to-cell-surface membrane traffic by binding to ARF and PtdIns(4)P. *Nat. Cell Biol.* **6,** 393–404
57. Wood, S. A., Park, J. E., and Brown, W. J. (1991) Brefeldin A causes a microtubule-mediated fusion of the trans-Golgi network and early endosomes. *Cell* **67,** 591–600
58. Gravotta, D., Deora, A., Perret, E., Oyanadel, C., Soza, A., Schreiner, R., Gonzalez, A., and Rodriguez-Boulan, E. (2007) AP1B sorts basolateral proteins in recycling and biosynthetic routes of MDCK cells. *Proc. Natl. Acad. Sci. U.S.A.* **104,** 1564–1569
59. Odorizzi, G., and Trowbridge, I. S. (1997) Structural requirements for basolateral sorting of the human transferrin receptor in the biosynthetic and endocytic pathways of Madin-Darby canine kidney cells. *J. Cell Biol.* **137,** 1255–1264
60. Dell'Angelica, E. C., Puertollano, R., Mullins, C., Aguilar, R. C., Vargas, J. D., Hartnell, L. M., and Bonifacino, J. S. (2000) GGAs. A family of ADP ribosylation factor-binding proteins related to adaptors and associated with the Golgi complex. *J. Cell Biol.* **149,** 81–94
61. Boman, A. L., Zhang, C. j., Zhu, X., and Kahn, R. A. (2000) A family of

ADP-ribosylation factor effectors that can alter membrane transport through the trans-Golgi. *Mol. Biol. Cell* **11,** 1241–1255
62. Hirst, J., Lui, W. W., Bright, N. A., Totty, N., Seaman, M. N., and Robinson, M. S. (2000) A family of proteins with γ-adaptin and VHS domains that facilitates trafficking between the trans-Golgi network and the vacuole/lysosome. *J. Cell Biol.* **149,** 67–80
63. Kuai, J., and Kahn, R. A. (2002) Assays of ADP-ribosylation factor function. *Methods Enzymol.* **345,** 359–370
64. Nakayama, K., and Takatsu, H. (2005) Analysis of Arf interaction with GGAs *in vitro* and *in vivo*. *Methods Enzymol.* **404,** 367–377
65. Yoon, H. Y., Bonifacino, J. S., and Randazzo, P. A. (2005) *In vitro* assays of Arf1 interaction with GGA proteins. *Methods Enzymol.* **404,** 316–332
66. Zhu, Y., Drake, M. T., and Kornfeld, S. (1999) ADP-ribosylation factor 1-dependent clathrin-coat assembly on synthetic liposomes. *Proc. Natl. Acad. Sci. U.S.A.* **96,** 5013–5018
67. Montagnac, G., de Forges, H., Smythe, E., Gueudry, C., Romao, M., Salamero, J., and Chavrier, P. (2011) Decoupling of activation and effector binding underlies ARF6 priming of fast endocytic recycling. *Curr. Biol.* **21,** 574–579
68. Díaz, E., and Pfeffer, S. R. (1998) TIP47. A cargo selection device for mannose 6-phosphate receptor trafficking. *Cell* **93,** 433–443
69. Medigeshi, G. R., and Schu, P. (2003) Characterization of the *in vitro* retrograde transport of MPR46. *Traffic* **4,** 802–811
70. Takatsu, H., Yoshino, K., and Nakayama, K. (2000) Adaptor γ ear homology domain conserved in γ-adaptin and GGA proteins that interact with γ-synergin. *Biochem. Biophys. Res. Commun.* **271,** 719–725
71. Hirst, J., Sahlender, D. A., Choma, M., Sinka, R., Harbour, M. E., Parkinson, M., and Robinson, M. S. (2009) Spatial and functional relationship of GGAs and AP-1 in *Drosophila* and HeLa cells. *Traffic* **10,** 1696–1710
72. Cai, H., Reinisch, K., and Ferro-Novick, S. (2007) Coats, tethers, Rabs, and SNARES work together to mediate the intracellular destination of a transport vesicle. *Dev. Cell* **12,** 671–682
73. Le Borgne, R., Schmidt, A., Mauxion, F., Griffiths, G., and Hoflack, B. (1993) Binding of AP-1 Golgi adaptors to membranes requires phosphorylated cytoplasmic domains of the mannose 6-phosphate/insulin-like growth factor II receptor. *J. Biol. Chem.* **268,** 22552–22556
74. Valdivia, R. H., Baggott, D., Chuang, J. S., and Schekman, R. W. (2002) The yeast clathrin adaptor protein complex 1 is required for the efficient retention of a subset of late Golgi membrane proteins. *Dev. Cell* **2,** 283–294
75. Meyer, C., Zizioli, D., Lausmann, S., Eskelinen, E. L., Hamann, J., Saftig, P., von Figura, K., and Schu, P. (2000) μ1A-adaptin-deficient mice. Lethality, loss of AP-1 binding, and rerouting of mannose 6-phosphate receptors. *EMBO J.* **19,** 2193–2203
76. Mallard, F., Antony, C., Tenza, D., Salamero, J., Goud, B., and Johannes, L. (1998) Direct pathway from early/recycling endosomes to the Golgi apparatus revealed through the study of shiga toxin B-fragment transport. *J. Cell Biol.* **143,** 973–990
77. Wahle, T., Prager, K., Raffler, N., Haass, C., Famulok, M., and Walter, J. (2005) GGA proteins regulate retrograde transport of BACE1 from endosomes to the trans-Golgi network. *Mol. Cell. Neurosci.* **29,** 453–461
78. Puertollano, R., and Bonifacino, J. S. (2004) Interactions of GGA3 with the ubiquitin sorting machinery. *Nat. Cell Biol.* **6,** 244–251
79. He, X., Li, F., Chang, W.-P., and Tang, J. (2005) GGA proteins mediate the recycling pathway of memapsin 2 (BACE). *J. Biol. Chem.* **280,** 11696–11703
80. Tesco, G., Koh, Y. H., Kang, E. L., Cameron, A. N., Das, S., Sena-Esteves, M., Hiltunen, M., Yang, S. H., Zhong, Z., Shen, Y., Simpkins, J. W., and Tanzi, R. E. (2007) Depletion of GGA3 stabilizes BACE and enhances β-secretase activity. *Neuron* **54,** 721–737
81. Pulvirenti, T., Giannotta, M., Capestrano, M., Capitani, M., Pisanu, A., Polishchuk, R. S., San Pietro, E., Beznoussenko, G. V., Mironov, A. A., Turacchio, G., Hsu, V. W., Sallese, M., and Luini, A. (2008) A traffic-activated Golgi-based signalling circuit coordinates the secretory pathway. *Nat. Cell Biol.* **10,** 912–922
82. McKay, M. M., and Kahn, R. A. (2004) Multiple phosphorylation events regulate the subcellular localization of GGA1. *Traffic* **5,** 102–116
83. Vieira, S. I., Rebelo, S., Domingues, S. C., da Cruz e Silva, E. F., and da Cruz e Silva, O. A. (2009) Ser-655 phosphorylation enhances APP secretory traffic. *Mol. Cell Biochem.* **328,** 145–154
84. D'Angelo, G., Polishchuk, E., Di Tullio, G., Santoro, M., Di Campli, A., Godi, A., West, G., Bielawski, J., Chuang, C. C., van der Spoel, A. C., Platt, F. M., Hannun, Y. A., Polishchuk, R., Mattjus, P., and De Matteis, M. A. (2007) Glycosphingolipid synthesis requires FAPP2 transfer of glucosylceramide. *Nature* **449,** 62–67
85. Calhoun, B. C., and Goldenring, J. R. (1996) Rab proteins in gastric parietal cells. Evidence for the membrane recycling hypothesis. *Yale J. Biol. Med.* **69,** 1–8